Sustainable Energy, Grids and Networks 43 (2025) 101850

Contents lists available at ScienceDirect

Sustainable Energy, Grids and Networks

journal homepage: www.elsevier.com/locate/segan

Valuing distributed energy resources flexibility in an uncertain and risk-aware low-carbon power system planning context

Pablo Apablaza [a,*], Sebastián Püschel-Løvengreen [b], Rodrigo Moreno [c,d], Pierluigi Mancarella [a,e]

[a] Department of Electrical and Electronic Engineering, The University of Melbourne, Melbourne, Victoria, Australia
[b] EnergyAustralia, Melbourne, Australia
[c] Department of Electrical Engineering, University of Chile, Santiago, Chile
[d] Instituto Sistemas Complejos de Ingeniería (ISCI), Santiago, Chile
[e] School of Electrical and Electronic Engineering, The University of Manchester, Sackville Street, Manchester M13 9PL, UK

ARTICLE INFO

Keywords:
Distributed energy resources
Investment under uncertainty
Power system planning
Stochastic optimisation
Risk aversion

ABSTRACT

This paper studies the relationship between the operational demand-side flexibility provided by the centralised coordination of distributed energy resources (DER) and the mitigation of economic risks in long-term transmission planning. DER coordination could represent an alternative to utility-scale network investments, offering increased operational flexibility, faster deployment, and fewer social licence issues. However, significant uncertainty surrounds DER uptake due to regulation and challenging consumer engagement. A multi-stage Conditional Value-at-Risk (CVaR) scenario-based formulation is introduced to study the techno-economic value of DER coordination across uncertain scenarios and planners' risk aversion preferences. Using a multi-stage decision tree, we endogenously incorporate long-term planning uncertainties, including DER and renewable energy uptake, retirement of coal generation, fuel and capital costs, as well as lead times. Case studies using real scenarios from Australia's National Electricity Market (NEM) reveal that DER coordination could reduce expected total system costs by up to 11 % and CVaR by 14 %. Coordination could also lead to narrower investment portfolios across several scenarios, with transmission capacity reductions of up to 4 GW in later stages. In contrast, a system lacking DER coordination faces poorer economic performance and a heightened risk of committing to inefficient investment paths, with reliance on high-capital investments increasing by up to 50 % of installed capacity.

1. Introduction

1.1. Background and motivation

Electric power systems worldwide are experiencing rapid growth in DER, driven by a combination of techno-economic factors, policy initiatives, and sustainability goals [1]. Notably, controllable DER, such as distributed battery storage systems, electric vehicles, and smart appliances, can provide important flexibility services by adjusting their power exchanges with the grid [2–4]. In fact, flexibility services provided by coordinated DER, e.g., via virtual power plants (VPP) [5], could contribute to power system planning by unlocking higher shares of variable renewable energy (VRE) [6], reshaping consumption patterns, reducing peak demand, and potentially delaying or deferring large-scale network investments [7]. Acknowledging this potential and its benefits, various system planners and policymakers are considering substantial DER uptake in their future scenarios. For example, Australia's Integrated System Plan (ISP) [8] anticipates approximately 30 GW of dispatchable DER battery storage by 2050, highlighting the economic benefits of adequate and timely coordination. However, from a long-term system planning perspective, there are important considerations regarding the integration of DER as a source of operational demand-side flexibility:

(I) Achieving a desired level of demand-side flexibility is deeply uncertain, depending on factors such as policy, regulation and consumer engagement. Explicitly considering DER uptake uncertainties in long-term investment plans could mitigate risks of over- or under-estimations. Nevertheless, decision-makers typically rely on deterministic approaches that fail to identify optimal investment strategies under uncertainty [9]. Methodological developments that incorporate these uncertainties in a multi-stage setting could lead to robust and adaptive portfolios, more capable of

* Corresponding author.
Email address: papablaza@student.unimelb.edu.au (P. Apablaza).

https://doi.org/10.1016/j.segan.2025.101850
Received 15 December 2024; Received in revised form 28 March 2025; Accepted 23 July 2025
Available online 30 July 2025

Nomenclature

Variables and functions: CVaR objective function formulation

$\boldsymbol{X}_n^{\mathrm{op}}$	$\forall n \in \mathcal{N}$, Vector of operational decisions
$\boldsymbol{X}_n^{\mathrm{inv}}$	$\forall n \in \mathcal{N}$, Vector of investment decisions
χ_ψ	$\forall \psi \in \Psi$, Auxiliary variable
λ	Value-at-risk (VaR)
$\mathrm{CVaR}_{1-\alpha}$	Conditional Value-at-Risk for shortfall probability $1-\alpha$
$\mathbb{E}[\mathbf{TC}]$	Expected total system cost
$\mathbf{TC}_{n/\psi}$	$\forall n \in \mathcal{N}$, Total cost for node n / scenario ψ
$\mathbf{C}_n^{\mathrm{op}}$	$\forall n \in \mathcal{N}$, Operational cost for node n of the scenario tree
$\mathbf{C}_n^{\mathrm{inv}}$	$\forall n \in \mathcal{N}$, Investment cost for node n of the scenario tree
$\mathbb{P}_\psi$	$\forall \psi \in \Psi$, Probability of scenario ψ

Investment decisions: $\forall n \in \mathcal{N}$

$x_{n,\hat{l}}^{\mathrm{L}}, \forall \hat{l} \in \hat{\mathcal{L}}$	Decision to invest in transmission line $\hat{l}$
$z_{n,\hat{l}}^{\mathrm{L}}, \forall \hat{l} \in \hat{\mathcal{L}}$	Availability of candidate transmission line $\hat{l}$

Operational decisions: $\forall n \in \mathcal{N}, t \in \mathcal{T}_w, w \in \mathcal{W}_n$

$e_{n,d,t}^{\mathrm{sh/shup/shdn}}$	$\forall d \in \mathcal{D}$, DER state of power shift/shift-up/-down (MWh)
$e_{n,e,t}^{\mathrm{E}}$	$\forall e \in \mathcal{E}$, Energy storage state of charge (MWh)
$f_{n,l,t}$	$\forall l \in \mathcal{L}$, Transmission line power flow (MW)
$f_{n,l,t}^{\mathrm{p/n}}$	$\forall l \in \mathcal{L}$, Transmission line positive/negative slack (MW)
$LS_{n,b,t}$	$\forall b \in \mathcal{B}$, Load shedding (MW)
$n_{n,g,t}$	$\forall g \in \mathcal{G}$, Number of online units in each gen.
$p_{n,g,t}$	$\forall g \in \mathcal{G}$, Conventional gen. power output (MW)
$p_{n,r,t}$	$\forall r \in \mathcal{R}$, Renewable gen. power output (MW)
$p_{n,r,t}^{\mathrm{c}}$	$\forall r \in \mathcal{R}$, Renewable gen. power curtailment (MW)
$p_{n,e,t}^{\mathrm{ch/dch}}$	$\forall e \in \mathcal{E}$, Energy storage charging/discharging power (MW)
$p_{n,g,t}^{s^{ty}}$	$\forall g \in \mathcal{G}$, Allocation of power for reserve s, type ty (MW)
$p_{n,e,t}^{s^{ty}}$	$\forall e \in \mathcal{E}$, Allocation of power for reserve s, type ty (MW)
$\gamma_{n,d,t}^{\mathrm{shup/shdn}}$	$\forall d \in \mathcal{D}$, DER power shift-up/shift-down (MW)
$\gamma_{n,d,t}^{\mathrm{red}}$	$\forall d \in \mathcal{D}$, DER power reduction (MW)
$\delta_{n,g,t}^{\mathrm{sdn/sup}}$	$\forall g \in \mathcal{G}$, Gen. shutdown/startup
$\Delta p_{n,a,t}^{\mathrm{g\text{-}loss}}$	$\forall a \in \mathcal{A}$, Generation contingency size for each area (MW)
$\kappa_{n,d,t}$	$\forall d \in \mathcal{D}$, DER power exchanges (MW)
$\mu_{n,e,t}$	$\forall e \in \mathcal{E}$, Energy storage state of operation (charge/discharge)
$\nu_{n,g,t}$	$\forall g \in \mathcal{G}$, Gen. power-on/off status
$\Omega_{n,a,t}^{s^{ty}}$	$\forall a \in \mathcal{A}$, Area allocation of power, reserve s, type ty (MW)

Parameters

$c_{n,g}^{\mathrm{fuel}}$	Gen. fuel cost ($/MW)
$c_g^{\mathrm{sup/sdn}}$	Gen. startup/shutdown cost ($)
$c_d^{\mathrm{shup/shdn}}$	DER load shift up/down cost ($/MW)
c_d^{red}	DER load reduction cost ($/MW)
$D_{n,b,w,t}$	Hourly power demand (MW)
$\bar{E}_e/\underline{E}_e$	Storage energy max./min. capacity (MWh)
$\bar{F}_{l,t}/\underline{F}_{l,t}$	Transmission line max. forward/reverse cap. (MW)
$\mathscr{F}_g/\mathscr{P}_g$	Gen. full/partial outage rate (%)
$\mathrm{LL}_{n,a}$	Largest possible area load loss (MW)
NT	Number of hours per representative period
$\mathrm{N}_{n,g}$	Max. number of online gen. units
$\bar{P}_g/\underline{P}_g$	Gen. max./min. power output (MW)
$\bar{P}_g^{\mathrm{pr/sr}^+}$	Gen. max. capacity for providing PR/SR (MW)
$\bar{P}_e^{\mathrm{ch/dch}}$	ESS max. charging/discharging power (MW)
$\bar{P}_e^{\mathrm{pr}}$	ESS max. cap. for primary reserves (MW)
$\bar{P}_{n,r,t}^{\mathrm{R}}$	Max. renewable gen. output (MW)
r	Financial discount rate (%)
$\mathrm{R}_g^{\mathrm{up/down}}$	Gen. up/downward ramp limit(MW)
RS_g	Gen. primary reserve slope
$\mathrm{T}_g^{\mathrm{up/dn}}$	Gen. min. up/down times (h)
$\mathrm{T}_g^{\mathrm{sup/sdn}}$	Gen. startup/shutdown times (h)
$\mathrm{T}^{\mathrm{pr/sr}}$	Time for primary/secondary reserve provision (s)
$\mathrm{T}_d^{\mathrm{rec}}$	DER re-balance time duration for load shift (h)
VoLL	Value of Lost Load ($ A/MW)
y_n	Number of years from node n to root node
$\bar{z}_{n,\hat{l}}^{\mathrm{L}}$	Max. capacity for line investment
$\bar{z}_{n,d}^{\mathrm{D}}$	DER available units
$1-\alpha$	Shortfall probability
β	Risk aversion weight
$\bar{\gamma}_d^{\mathrm{shup/shdn}}$	DER max. up/down load shifting capacity (MW)
$\bar{\gamma}_d^{\mathrm{red}}$	DER max. load reduction capacity (MW)
$\Gamma_{n,h,w}$	Hydro gen. historical inflows
Δf^{db}	Freq. response deadband target deviation (Hz)
$\Delta f^{\mathrm{qssf}^{-/+}}$	Target QSS frequency low/high events (Hz)
ζ_d	DER payback effect penalisation (%)
$\eta_e^{\mathrm{ch/dch}}$	Storage charging/discharging efficiency (%)
$\tilde{\kappa}_{n,\tilde{d},t}$	DER reference power (MW)
$\Xi_{n,h,w}$	Hydro gen. capacity factor (%)
$\pi_{n,\hat{l}}^{\mathrm{L}}$	Annuitised transmission line investment cost ($)
ρ_n	Probability of node n
σ_a	Area load damping factor (%/Hz)
υ_g	Gen. derating factor due to partial outage
ω_w	Representative period relative yearly weight

Acronyms

AEMO	Australian Energy Market Operator
CVaR	Conditional Value-at-Risk
DER	Distributed energy resources
ESS	Energy storage system
ISP	Integrated System Plan
NEM	National Electricity Market
QSS	Quasi steady state
QSSF	Quasi steady state frequency
VaR	Value-at-Risk
VPP	Virtual Power Plant
VRE	Variable Renewable Energy

hedging against economic risks associated with DER coordination [7,10].

(II) Large-scale investments like transmission lines carry significant economic risks due to supply chain constraints or social licence issues, which could lead to increased capital costs and extended construction times. Flexible technologies that enhance the management of peak and net load could help mitigate these risks by delaying or preventing their construction, avoiding lock-in to suboptimal investment paths [11]. However, properly valuing synergies and trade-offs between DER flexibility and network investments under different scenarios requires an approach capable of measuring stakeholders' risk appetites. For instance, Australia's ISP [8] indicates that consumers would accept a level of risk aversion in infrastructure planning to protect against volatility in electricity bills.

(III) The transition to more decentralised power systems has complexified the interactions between an active demand side, highly variable renewable generation, and the transmission network. This shift requires investment decisions supported by thorough operational modelling. As [12] suggests, considering detailed operative constraints, such as ramping and operation of thermal units and VRE intermittency, as well as long-term uncertainties, is crucial for valuing flexible technologies in a DER-rich landscape.

1.2. Literature review

Given the background discussed above, this section reviews the key works that have contributed to this research area and outlines the primary literature gaps addressed in this paper.

From a systemic viewpoint, progressing towards DER coordination offers benefits but also poses significant challenges that must be carefully addressed. The authors in [13,14] conclude that proper DER management could reduce demand during peak hours, accommodate higher volumes of VRE and release latent capacity of existing transmission assets. Given these benefits and decreasing technology costs, planners in different jurisdictions [8,15–17] foresee substantial availability of demand-side flexibility in their long-term scenarios. Coordination and aggregation, for example, through virtual power plants (VPP) [5,18], emerge as a practical approach to exploit that flexibility in a centralised manner at various scales.

In the context of long-term transmission planning, diverse studies have investigated the impact and value streams of DER flexibility. For instance, in [19], through a distributionally robust approach, the authors demonstrate the potential of coordinated DER to replace inefficient network investments. Similarly, the research conducted in [20] illustrates how DER could bolster system resilience against extreme events while reducing network investments that might become stranded. In [21], the authors solve a non-linear optimisation problem to study the impact of DER in planning, while [22] utilises a bi-level coordination framework. Both approaches conclude that DER flexibility offers significant value as a non-network alternative in planning.

Despite relevant research, a crucial aspect remains significantly understudied: the uncertainties associated with DER coordination and how these interact with the investments in the transmission system. The authors of [23] note that DER impacts on the bulk power system could fluctuate significantly due to uncertainty and varying controllability levels, indicating that further studies are necessary. To start addressing this, the authors in [7] showcase that modelling incorporating several simultaneous long-term uncertainties (e.g. DER, VRE and storage deployment, load growth, and fuel prices) could be crucial for capturing risk-hedging value from controllable DER. This approach would allow informing with more robust and anticipatory transmission system investment plans compared to deterministic methods.

Given these considerations, system planning under uncertainty has become crucial as multiple complex factors influence decisions about new transmission infrastructure. In [10,24], it is argued that a proactive, uncertainty-aware transmission planning paradigm is more suitable for decision-making, generating adaptive and anticipatory portfolios over time. Conversely, a deterministic (single-scenario) approach might overvalue network investments tailored to specific future conditions, potentially compromising system integrity and leaving it vulnerable to unforeseen scenarios.

Various studies have explored modelling approaches to address uncertainty in power system planning. Stochastic programming, robust optimisation, and robust decision-making have emerged as compelling alternatives to deterministic methods [25]. Notably, a comparative study revealed that stochastic frameworks could identify superior investment plans, particularly in reducing expected costs [26]. Advancements in stochastic programming for power system planning have made efforts to incorporate high-resolution uncertainty and operational models. Research in [12] demonstrates that including high-resolution operational constraints yields additional value from flexible technologies in a planning context. Similarly, the authors of [27] argue for a more nuanced representation of uncertainties within a decision tree. However, these advances do not fully address the role of DER, especially in light of varying levels of risk awareness, which is the focus of this paper.

Existing literature has proposed risk-aware planning models incorporating various metrics such as variance [28], shortfall probability, or Value-at-Risk (VaR) [29]. More recently, the optimisation of Conditional Value-at-Risk (CVaR) [30] has been integrated into planning under uncertainty using stochastic programming. Two-stage CVaR-constrained generation expansion planning is examined in [31,32], highlighting the implications of risk aversion and the role of a diverse generation portfolio in hedging against risks. Two-stage CVaR-based network planning has also been applied in [33–36], revealing strong non-linearities in the effects of investing in various technologies depending on the level of risk aversion.

Although important research exists in risk-aware expansion planning, there remains a critical gap in understanding how DER coordination and transmission network investments interact, especially when incorporating planners' risk attitudes across multiple investment stages. This challenge is compounded by the significant uncertainty in accessing demand-side flexibility through DER controllability, influenced by factors like policymaking and consumer preferences, requiring a comprehensive framework that can effectively address this and other long-run uncertainties. Furthermore, given that planners face recurring decisions about massive capital-intensive infrastructure investments, the ability to adjust risk aversion parameters for hedging against worst-case scenarios accurately becomes crucial to developing robust investment strategies that minimise the potential negative impacts of suboptimal investment decisions.

1.3. Contributions of this paper

Building upon the identified literature gaps, this paper presents a comprehensive multi-stage risk- and uncertainty-aware transmission network investment planning framework. The proposed approach incorporates detailed mathematical modelling of power system operation, including unit commitment constraints, reserve requirements, and coordinated DER flexibility services such as energy arbitrage, peak shaving, and load shifting. Risk assessment is integrated through a multi-stage CVaR-based formulation with a scenario total-cost loss function that is fully parameterisable by the ratio of risk aversion. Uncertainty is modelled via scenarios using a granular decision tree across various investment stages. The model employs hourly time steps over representative weeks to fully capture VRE, DER, and demand variability. A set of case studies based on real scenarios from the Australian Energy Market Operator (AEMO) studies and thoroughly demonstrates the potential techno-economic merits of DER coordination in the expansion of the transmission system under several long-run uncertainties and varying levels of stakeholder risk attitudes. To present our results, we employ a suite of techno-economic metrics to showcase the impacts and value of DER coordination in power system planning across different levels of risk aversion. Hence, the main contributions of this paper are:

- **Contribution #1**: A fully parameterisable multi-stage scenario-based CVaR linear formulation for power system planning incorporating a DER aggregation model that accounts for coordinated and non-coordinated modes. This formulation allows endogenously measuring planners' risk positions across several scenarios in order to optimise investment portfolios under uncertainty.
- **Contribution #2**: A thorough analysis of the synergies and trade-offs between transmission network investments and the coordination of DER in planning under uncertainty, demonstrating the techno-economic merits and limitations of both technologies across varying levels of planners' risk preferences.
- **Contribution #3**: An enhanced understanding of the potential ability of coordinated DER in contributing to handling economic risks emanating from threatening long-term planning uncertainties, such as building delays and increased capital costs due to supply chain constraints and social licence issues.

The remainder of this paper is structured as follows. Section 2 presents the risk-aware stochastic power system planning framework. Section 3 delves into the system data utilised and the case studies considered. Section 4 presents the results and discussion. Section 5 concludes.

2. Risk-aware multi-stage stochastic power system planning framework

This section presents the risk-aware multi-stage framework for power system planning under uncertainty to study the impact and value of DER demand-side flexibility. The section is divided into (1) the modelling of long-term uncertainties using a scenario tree, (2) the mathematical formulation to incorporate the CVaR of total operational and investment expenses for tail scenarios in a multi-stage and multi-scenario setting, and (3) a comprehensive power system operational modelling for planning, including detailed operative constraints such as unit commitment, reserve requirements, and demand-side flexibility services provided by coordinated DER.

2.1. Uncertainty modelling: multi-stage scenario tree

Modern power systems face significant uncertainty due to the increasing penetration of VRE, varying DER adoption and fuel prices, as well as other factors. To address these uncertainties in long-term planning, decision-makers typically develop a comprehensive set of plausible scenarios representing potential future states of the system under consideration. These scenarios often follow an incremental progression over varying levels of optimism regarding decarbonisation and technology uptake for uncertain parameters ξ_i, as illustrated in Fig. 1. Over these plausible scenarios, planners primarily utilise deterministic frameworks, producing tailored investment portfolios for each envisioned future state of the system and posteriorly deciding the best-performing plan based on specific criteria. However, these approaches have a significant drawback: it is challenging to establish a single investment plan that can adequately address a highly uncertain future. Hence, the goal is to develop an adaptable system expansion strategy that performs well across a broader range of unfolding futures.

To address this issue and endogenously incorporate multiple simultaneous uncertainties in the decision-making, we formulate the proposed model as a multi-stage stochastic problem. This approach reflects realistic decision-making patterns, specifically an adaptive investment schedule [9]. Thus, the planning problem is structured as a decision tree with $|\mathcal{S}|$ decision stages and $|\mathcal{N}|$ nodes, where $\mathcal{S}$ and $\mathcal{N}$ are the respective sets. Fig. 2 illustrates a multi-stage decision tree that creates incremental scenarios based on the uncertain parameters ξ_i depicted in Fig. 1. This tree provides a coherent description of the evolution of these parameters [11], enabling a comprehensive analysis of potential future outcomes.

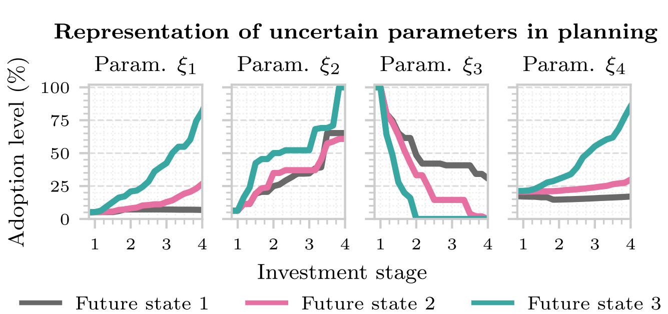

Fig. 1. Illustrative representation of the behaviour of uncertain parameters in power system planning from AEMO's ISP [37]. ξ_1 : solar PV deployment, ξ_2 : adoption of utility-scale storage, ξ_3 : participation of coal-fired units in the system, ξ_4 : load growth.

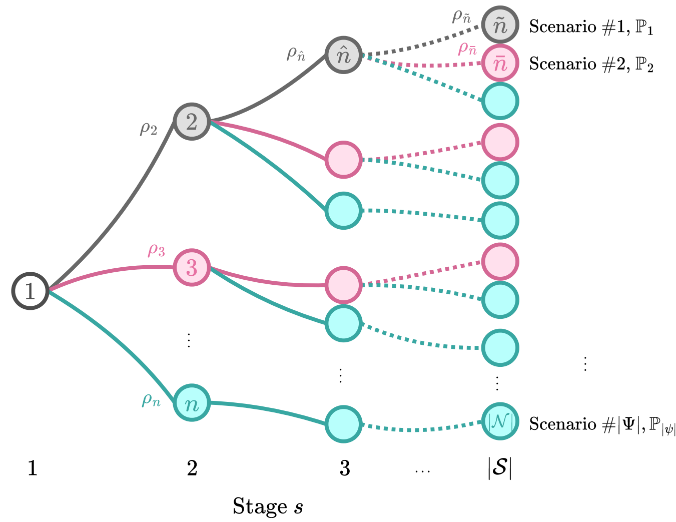

Fig. 2. Illustrative multi-stage scenario tree for power system planning with $|\mathcal{S}|$ stages, $|\mathcal{N}|$ nodes and $|\Psi|$ incremental scenarios. Incremental scenarios are created based on the information from Fig. 1.

Each node $n \subset \mathcal{N}$ in the decision tree contains a realisation of uncertain parameters ξ_i linked to a specific future, varying based on the central planner's assumptions (each colour in the tree represents a realisation of uncertain parameters at a given decision stage). We adopt an incremental scenario approach to enhance the level of uncertainty captured in the decision tree representation and identify the most valuable investment options [27]. This methodological approach combines the original future states of the system and creates intermediate scenarios (progressing from the "grey" state of the system to the "blue" state, as shown in Fig. 1), resulting in a total of $|\Psi|$ scenarios. Ψ is the set of all scenarios. Subsequently, each scenario $\psi \subseteq \Psi$ is formed by a set of nodes $\mathcal{N}_\psi$ following the "path" from a leaf node (located in stage $|\mathcal{S}|$) to the root node ($n = 1$). For instance, in the decision tree shown in Fig. 2, the path of scenario $\psi = 2$ comprises nodes $\mathcal{N}_{\psi=2} = \{1, 2, \hat{n}, \bar{n}\}$. The probability assigned to each scenario, $\mathbb{P}_\psi$, is then calculated as the product of the occurrence probabilities of its constituent nodes ρ_n, as expressed in (1):

$$\mathbb{P}_\psi = \prod_{n \in \mathcal{N}_\psi} \rho_n \tag{1}$$

In this scenario tree-based approach, each node comprises an operational and an investment phase. The investment phase determines infrastructure investments for the current node $\boldsymbol{X}_n^{\text{inv}}$ that become available in the current or subsequent stages, depending on the lead times of the asset. The operational phase determines the optimal system operation $\boldsymbol{X}_n^{\text{op}}$ for given values of the uncertain parameters. Hence, operational and investment decisions $\{\boldsymbol{X}_n^{\text{op}}, \boldsymbol{X}_n^{\text{inv}}\}$ at each node n in a specific stage s depend on both observed uncertain parameters ξ_i and previously committed infrastructure $\boldsymbol{X}_{\text{pre}(n)}^{\text{inv}}$,[1] enabling a proper valuation of various investment candidates.

2.2. Risk-aware mathematical formulation

In this section, we present the mathematical formulation that incorporates risk awareness in a multi-stage stochastic planning setting. Decision-makers typically aim to reduce expected costs while handling the risk of the resulting investment portfolio $\boldsymbol{X}^{\text{inv}}$. As illustrated in Fig. 3, decision-making in planning involves a trade-off between future costs and risks when uncertainty is present. For a set of investment options, the planner would ideally choose investments that reduce both total

[1] pre(n) is a function that returns the pre-node of node of n.

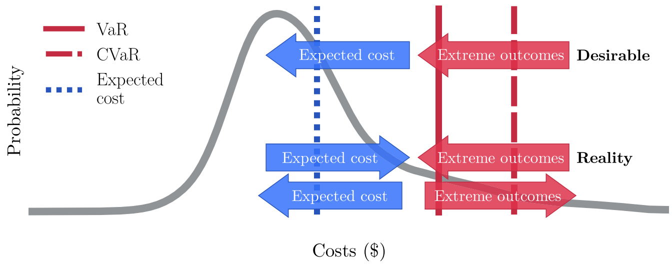

Fig. 3. Illustrative cost probability distribution to show possible outcomes when managing the risk of an investment portfolio in power system planning under uncertainty. It would be desirable to have a technological option capable of achieving a reduction in expected costs as well as extreme outcomes (e.g. measured via CVaR). However, the reality is that any option comes at a cost. Implementing a hedge to mitigate tail risks typically involves paying a premium, thereby increasing expected costs. Conversely, when expected costs are reduced through less infrastructure investment, the system becomes more vulnerable to extreme scenarios, thereby increasing their potential impact (measured as well via CVaR).

expected costs and worst-case outcomes (taken as a measure of risk) as uncertainty unfolds. In practice, with any fixed set of options, reducing extreme outcomes might require additional investments (a "risk hedge"), which increases the expected cost [38]. Conversely, attempts to lower the expected cost by investing in cheaper options typically lead to poorer performance (higher total costs) in certain scenarios. The emergence of new technologies might improve this cost-risk trade-off if they offer lower capital costs or enhance system operation through improved flexibility that reduces operational expenses. In this context, and without excluding other alternatives, DER coordination could exemplify such an option, as it leverages existing distributed assets while carrying fewer implementation risks than traditional transmission infrastructure, which faces substantial market and regulatory hurdles, potentially deriving into extended lead times, supply chain and social licence challenges.

Hence, we formulate the objective function based on the CVaR optimisation approach outlined in [30] to assess the role of flexible DER coordination in a risk-aware and uncertain planning context. For a given quantile α[2] of the total cost distribution, via an optimisation problem, we obtain the optimal investment portfolio for each node $n \in \mathcal{N}$ of the decision tree, $\boldsymbol{X}_n^{\text{inv}}$, the VaR λ, and $\text{CVaR}_{1-\alpha}$. We assume that the decision-maker minimises a multi-objective function (2), given by the β-weighted sum of the total expected system costs $\mathbb{E}[\mathbf{TC}]$ and the $\text{CVaR}_{1-\alpha}$ of the scenario cost distribution described by the scenario tree. Parameter β balances the risk position of the decision-maker. $\beta = 0$ corresponds to a risk-neutral assessment (expected cost minimisation), while $\beta = 1$ is a fully risk-averse approach (CVaR minimisation). Expected total system costs in (3) are given by the sum of total costs $\mathbf{TC}_n$ for each node n of the scenario tree. Total costs for each node (4), $\mathbf{TC}_n$, are the discounted probability-weighted sum of operational and investment costs, given by operational and investment decisions $\boldsymbol{X}_n^{\text{op}}, \boldsymbol{X}_n^{\text{inv}}$ over cost functions $\mathbf{C}_n^{\text{op}}, \mathbf{C}_n^{\text{inv}}$, respectively. r is the discount rate and y_n the years from node n to the root node. Performance of $\text{CVaR}_{1-\alpha}$ for quantile α is given by (5), where λ is the VaR of the distribution. We use the total costs for each scenario ψ, $\mathbf{TC}_\psi$, as a linear loss function, with the probability of each scenario given by $\mathbb{P}_\psi$. This approach is justified by the multi-stage nature of the scenario tree, where each scenario ψ (following a path from a leaf node to the root node) has a likelihood $\mathbb{P}_\psi$. This allows the creation of a discrete probability distribution of total scenario costs, measured in constraint (6) via auxiliary variable χ_ψ, to determine the VaR (λ), and consequently minimising $\text{CVaR}_{1-\alpha}$ and system costs.

[2] The probability that total costs exceed the VaR λ equals to $1-\alpha$, also known as "shortfall probability".

Model: Multi-stage CVaR objective function formulation

Sets and indices:

$n \in \mathcal{N}$	Nodes in the scenario tree
$\psi \in \Psi$	Scenarios in the scenario tree

Objective function:

$$\min_{\boldsymbol{X}_n^{\text{op}}, \boldsymbol{X}_n^{\text{inv}}} (1-\beta) \cdot \mathbb{E}[\mathbf{TC}] + \beta \cdot \text{CVaR}_{1-\alpha} \tag{2}$$

CVaR constraints:

$$\mathbb{E}[\mathbf{TC}] = \textstyle\sum_{n \in \mathcal{N}} \mathbf{TC}_n \tag{3}$$

$$\mathbf{TC}_n = \frac{\rho_n}{(1+r)^{y_n}} \left(\mathbf{C}_n^{\text{op}}(\boldsymbol{X}_n^{\text{op}}) + \mathbf{C}_n^{\text{inv}}(\boldsymbol{X}_n^{\text{inv}}) \right) \tag{4}$$

$$\text{CVaR}_{1-\alpha} = \lambda + \frac{1}{1-\alpha} \cdot \textstyle\sum_{\psi \in \Psi} \mathbb{P}_\psi \cdot \chi_\psi \tag{5}$$

$$\mathbf{TC}_\psi - \lambda \leq \chi_\psi \forall \psi \in \Psi \tag{6}$$

$$\mathbf{TC}_\psi = \textstyle\sum_{n \in \mathcal{N}_\psi} \mathbf{C}_n^{\text{op}}(\boldsymbol{X}_n^{\text{op}}) + \mathbf{C}_n^{\text{inv}}(\boldsymbol{X}_n^{\text{inv}}) \tag{7}$$

2.3. Operation and investment modelling for planning

This section outlines the operation and investment modelling for the risk-aware power system planning framework. We include constraints to represent realistic investment behaviour, such as infrastructure lead times, as well as detailed short-term operational constraints like unit commitment, reserves for managing short-term uncertainty, storage operation, and coordinated DER flexibility services. The investment cost function $\mathbf{C}_n^{\text{inv}}$ described by (8) for each node n of the scenario tree is given by the sum of the annuities $\pi_{n,\hat{l}}^{\text{L}}$ paid for new transmission lines if the decision $x_{n,\hat{l}}^{\text{L}}$ is made to invest in them. The operational cost function $\mathbf{C}_n^{\text{op}}$ (9) is given by the operation of the system over a set of representative weeks $\mathcal{W}_n$ weighted by ω_w for each node n. Operational cost includes fuel $c_{n,g,t}^{\text{fuel}}$, start-up $c_{n,g,t}^{\text{sup}}$ and shut-down $c_{n,g,t}^{\text{sdn}}$ of synchronous units, coordinated DER services (load shifting $c_{n,\tilde{e},t}^{\text{shup/shdn}}$ and reduction $c_{n,g,t}^{\text{red}}$). Load shedding in each bus b is measured by $LS_{n,b,t}$ and penalised with the Value of Lost Load (VoLL).

The construction of new transmission lines is modelled through non-anticipativity constraints (10), which ensure that an investment made at a node n in the scenario tree is irreversible and remains consistent across all scenarios. These constraints also limit the number of new units installed at each node. The lead time for transmission lines includes a one-stage delay between the investment decision $x_{n,\hat{l}}^{\text{L}}$ and the asset's availability $z_{n,\hat{l}}^{\text{L}}$. As a result, new lines cannot be installed in the first investment stage (root node of the scenario tree, $n = 1$) as specified in (11). Additionally, the payment of annuities begins one stage before the asset becomes available. Investment variables for transmission lines are binary to represent real projects, as imposed in (12).

Eq. (13) ensures power balance between supply and demand at every bus b at each hour t, for each representative period w and node n. Outputs from conventional generation $p_{n,\tilde{g},t}$ and renewable generation $p_{n,\tilde{r},t}$, power flows through lines $f_{n,\tilde{l},t}$, and energy exchanges of storage systems $p_{n,\tilde{e},t}^{\text{ch/dch}}$ meet requirements of the demand side at each bus b. Demand side comprises inflexible demand $D_{n,b,w,t}$ and DER operation. Variable $\kappa_{n,d,t}$ allows modelling power exchanges of non-coordinated or coordinated DER modes. The latter provides flexibility services in an aggregated fashion.

Each synchronous unit (including hydro) is modelled through (14)–(18). These units can provide primary (pr) and secondary (sr) upward (+) and downward (-) reserves during high- and low-frequency events, represented by reserve allocation variables $p_{n,g,r}^{\text{pr/sr}^\pm}$. Eq. (14) describes minimum generation and downward reserves, with a lower bound set by the number of online units $n_{n,g,t}$ and minimum power output $\underline{P}_g$. Maximum generation and upward (+) reserves are described by (15)–(17), limited by the maximum output of units $\bar{P}_g$ and reserve limits

Model: Operational and investment modelling for power system planning (A)

Sets and indices:

$a, b \in \mathcal{A}, \mathcal{B}$	Areas, buses in the system
$d, \tilde{d} \in \mathcal{D}, \mathcal{D}_b$	DER in the system, in bus b
$e, \tilde{e}, \bar{e} \in \mathcal{E}, \mathcal{E}_b, \mathcal{E}_a$	ESS in the system, in bus b, in area a
$g \in \mathcal{G}$	Synchronous generators in the system
$\tilde{g}, \bar{g} \in \mathcal{G}_b, \mathcal{G}_b$	Synchronous generators in bus b, in area a
$h \in \mathcal{G}^{\mathrm{H}} \subset \mathcal{G}$	Hydro generators in the system
$l \in \mathcal{L}$	Transmission lines in the system
$\tilde{l} \in \mathcal{L}^{\mathrm{from}}_b, \mathcal{L}^{\mathrm{to}}_b$	Transmission lines from, to bus b
$\hat{l} \in \hat{\mathcal{L}} \subset \mathcal{L}$	Candidate transmission lines
$m \in \mathcal{P}_n$	Predecessor nodes of node n (including n)
$r, \tilde{r} \in \mathcal{R}, \mathcal{R}_b$	Variable renewable gen. in the system, bus b
$t \in \mathcal{T}_w$	Hours within a representative period w
$w \in \mathcal{W}_n$	Representative periods in node n

Cost functions:

$$\mathbf{C}^{\mathrm{inv}}_n(\boldsymbol{X}^{\mathrm{inv}}_n) = \sum_{\hat{l}\in\mathcal{L}^{\mathrm{c}}} \pi^{\mathrm{L}}_{n,\hat{l}}(x^{\mathrm{L}}_{n,\hat{l}} + z^{\mathrm{L}}_{n,\hat{l}}) \quad (8)$$

$$\mathbf{C}^{\mathrm{op}}_n(\boldsymbol{X}^{\mathrm{op}}_n) = \sum_{b\in\mathcal{B}} \sum_{w\in\mathcal{W}_n} \sum_{t\in\mathcal{T}_w} \omega_w \Big(\sum_{\tilde{g}\in\mathcal{G}_b} \Big(c^{\mathrm{fuel}}_{n,\tilde{g}} p_{n,\tilde{g},t} + c^{\mathrm{sup}}_{\tilde{g}} \delta^{\mathrm{sup}}_{n,\tilde{g},t} + c^{\mathrm{sdn}}_{\tilde{g}} \delta^{\mathrm{sdn}}_{n,\tilde{g},t} \Big) + \sum_{\tilde{d}\in\mathcal{D}_b} \Big(c^{\mathrm{shup}}_{\tilde{d}} \gamma^{\mathrm{shup}}_{n,\tilde{d},t} + c^{\mathrm{shdn}}_{\tilde{d}} \gamma^{\mathrm{shdn}}_{n,\tilde{d},t} + c^{\mathrm{red}}_{\tilde{d}} \gamma^{\mathrm{red}}_{n,\tilde{d},t} \Big) + \mathrm{VoLL} \cdot LS_{n,b,t} \Big) \quad (9)$$

Investment constraints:

$$z^{\mathrm{L}}_{n,\hat{l}} \le \textstyle\sum_{m\in\mathcal{P}_n} x^{\mathrm{L}}_{m,\hat{l}} \le \bar{z}^{\mathrm{L}}_{n,\hat{l}}, \forall n, \hat{l} \quad (10)$$

$$z^{\mathrm{L}}_{1,\hat{l}} = 0, \forall \hat{l} \quad (11)$$

$$x^{\mathrm{L}}_{n,\hat{l}}, z^{\mathrm{L}}_{n,\hat{l}} \in \{0,1\}, \forall n, \hat{l} \quad (12)$$

Balance equation: $\forall n \in \mathcal{N}, b \in \mathcal{B}, w \in \mathcal{W}_n, t \in \mathcal{T}_w$

$$\sum_{\tilde{g}\in\mathcal{G}_b} p_{n,\tilde{g},t} + \sum_{\tilde{r}\in\mathcal{R}_b} p_{n,\tilde{r},t} + \sum_{\tilde{l}\in\mathcal{L}^{\mathrm{to}}_b} f_{n,\tilde{l},t} - \sum_{\tilde{l}\in\mathcal{L}^{\mathrm{from}}_b} f_{n,\tilde{l},t} + \sum_{\tilde{e}\in\mathcal{E}_b} \Big(p^{\mathrm{dch}}_{n,\tilde{e},t} - p^{\mathrm{ch}}_{n,\tilde{e},t} \Big) = D_{n,b,w,t} - LS_{n,b,t} + \sum_{\tilde{d}\in\mathcal{D}_b} \kappa_{n,\tilde{d},t} \quad (13)$$

$\bar{P}^{\mathrm{pr/sr^+}}_g$, respectively. Reserve slope RS_g limits the headroom as a generator approaches its maximum capacity. Eq. (18) accounts for maximum generation, considering outage rates computed using full $\mathscr{F}_g$ and partial $\mathscr{P}_g$ outage rates, as well as the derating factor υ_g due to partial outage of a generator. For renewable units, (19) ensures the available renewable resource at time t, $\tilde{P}^{\mathrm{R}}_{n,r,t}$ is balanced between injections $p_{n,r,t}$ and curtailed power $p^{\mathrm{c}}_{n,r,t}$. Eq. (20) presents maximum run-of-river generation, limited by historical inflow data $\Gamma_{n,h,w}$, while (21) uses hydro unit capacity factors $\Xi_{n,h,w}$ to constrain energy generation from reservoirs. NT is the total number of hours within a representative period.

The operation of storage systems (ESS), such as battery storage (BESS), pumped hydro storage (PHES), and virtual power plants (VPP), is described in (22)–(30). Integer variable $\mu_{n,e,t}$ determines power consumption or injection in (22) and (23), limited by maximum values $\bar{P}^{\mathrm{ch/dch}}_e$. Eqs. (24) and (25) model the allocation of primary and secondary upward and downward reserves provided by ESS using variables $p^{\mathrm{pr/sr^{\pm}}}_{n,g,r}$. Eq. (26) sets the maximum level of primary reserves (pr), limited by parameter $\bar{P}^{\mathrm{pr}}_e$. Energy balance of storage, measured at every time step by variable $e^{\mathrm{E}}_{n,e,t}$, is described in (27) using efficiency parameters for charging and discharging, $\eta^{\mathrm{ch/dch}}_e$, and bounded by capacity limits $\underline{E}_e, \bar{E}_e$ in (28). Eqs. (29) and (30) ensure the storage unit has sufficient energy capacity to provide reserves for the duration $\mathrm{T}^{\mathrm{pr}}, \mathrm{T}^{\mathrm{sr}}$ required in primary and secondary reserve services. VPPs do not provide reserves.

The operation of coordinated DER is modelled in an aggregated fashion, enabling them to offer local flexibility services via (31)–(35) in each bus of the system. Eq. (31) captures DER hourly power exchanges. Input parameter $\tilde{\kappa}_{n,d,t}$ represents inflexible exchanges (independent of market signals). Variables $\gamma^{\mathrm{shup/shdn}}_{n,d,t}$ and $\gamma^{\mathrm{red}}_{n,d,t}$ model the active power exchanges of load shifting and reduction DER services. For a non-coordinated DER mode, these decision variables are omitted. Eqs. (32) and (33) model load shifting, allowing for a reduction in energy consumption at a given time and shifting to times when energy could be more economical. Eq. (32) tracks power shift up and down exchanges, while (33) restricts load rebalancing to occur every $\mathrm{T}^{\mathrm{rec}}_d$ periods. Parameter ζ_d accounts for the payback effect [39], reflecting the interplay between physical characteristics of appliances and flexible consumption patterns. DER modelling also integrates load reduction services (peak shaving), representing devices that reduce power consumption as a form of demand response. Eqs. (31) and (35) model this service, which is priced with $c^{\mathrm{red}}_{\tilde{d}}$ in the operational cost function (9) as payment to the customer for unconsumed energy. Eq. (35) limits the power exchange capacity for each DER service. As transmission system planners do not directly influence decisions in distribution networks, investment in new DER is out of the scope of this work.

Transmission lines are modelled using a fully dispatchable transport approach. Forward $\bar{F}_{l,t}$ and reverse $\underline{F}_{l,t}$ capacities of lines are represented in (36). Variable $z^{\mathrm{L}}_{n,l}$ determines the line's availability based on whether it's an existing asset or an investment candidate. Eqs. (37) and (38) define the transmission headroom in each direction, using variables $f^{\mathrm{p}}_{n,l,t}$ for positive (forward) headroom and $f^{\mathrm{n}}_{n,l,t}$ for negative (reverse) headroom.

Unit commitment constraints (39)–(45) for synchronous generators [40] model the scheduling of units, ramp limits, startup, shutdown, and minimum on-off times. Eq. (39) describes the number of online units in each period and the startup-shutdown transitions. Variables $\delta^{\mathrm{sdn/sup}}_{n,g,t}$ model the shutdown/startup of each unit in generator g. Minimum up-times $\mathrm{T}^{\mathrm{up}}_g$ and down-times $\mathrm{T}^{\mathrm{dn}}_g$ are ensured through (40) and (41), respectively. $\mathrm{N}_{n,g}$ represents the maximum number of online units for generator g, which varies depending on the scenario associated with node n, due to retirements of coal-fired units. Eq. (41) incorporates startup $\mathrm{T}^{\mathrm{sup}}_g$ and shutdown $\mathrm{T}^{\mathrm{sdn}}_g$ transition times. Each cluster of units changes its output between successive periods, limited by the unit's ramping ability $\mathrm{R}^{\mathrm{up/down}}_g$ and the units that may become active or inactive in the interval. Eq. (42) represents a generator's upward change in output, considering the ramping capability of units and those becoming active in that period. Eq. (43) describes the generator's maximum downward output change based on the units' ramping and shutdown. Eq. (44) ensures the units turned on in each generator do not exceed the maximum available $\mathrm{N}_{n,g}$. By using variable $\nu_{n,g,t}$, which models the power-on of generators, (45) limits the number of units that can be committed relative to the total available units for each online generator g. To reduce the computational burden associated with integer variables, $n_{n,g,t}, \nu_{n,g,t}, \delta^{\mathrm{sup}}_{n,g,t}, \delta^{\mathrm{sdn}}_{n,g,t}$ can be relaxed by grouping generation units of similar characteristics without introducing substantial errors [40].

Eqs. (46) and (47) define, through variables $\Omega^{\mathrm{pr/sr}^{ty}}_{n,a,t}$, the total allocation of reserves for primary and secondary services of type ty (upward and downward) in each area a of the system. Reserves are the sum of those provided by generators and storage. The determination of contingency size for both generation $\Delta p^{\mathrm{g\text{-}loss}}_{n,a,t}$ and load $\bar{D}_{n,a,t}$ is conducted for each area, allowing for granular reserve allocation. Eq. (48) defines the largest loss of generation, while (49) determines the largest load contingency for each area and period t, respectively. The load contingency value $\mathrm{LL}_{n,a,t}$ must be an input parameter for the problem, as the unit commitment modelling does not consider demand dispatch. Quasi-steady-state frequency (QSSF) constraints, given by (50) and (51), ensure sufficient local primary reserves (pr) in each system area to reach the QSSF for load or generation losses. $\Delta f^{\mathrm{qssf}^{-/+}}$ is the target QSS frequency for low/high events, while σ_a is the load damping factor in each area. Secondary reserves (sr) are allocated through constraints (52) and (53) for each area and event type (low or high), aiming to bring the frequency back to the dead band. Δf^{db} is the frequency response deadband target deviation.

Model: Operational and investment modelling for power system planning (B)

Generator limits: $\forall n \in \mathcal{N}$

$$n_{n,g,t}\underline{P}_g \le p_{n,g,t} - p^{\mathrm{pr}^-}_{n,g,t} - p^{\mathrm{sr}^-}_{n,g,t}, \forall g,t \tag{14}$$

$$p_{n,g,t} + \frac{p^{\mathrm{pr}^+}_{n,g,t}}{\mathrm{RS}_g} + p^{\mathrm{sr}^+}_{n,g,t} \le n_{n,g,t}\bar{P}_g, \forall g,t \tag{15}$$

$$p^{\mathrm{pr}^+}_{n,g,t} \le n_{n,g,t}\bar{P}^{\mathrm{pr}^+}_g, \forall g,t \tag{16}$$

$$p^{\mathrm{sr}^+}_{n,g,t} \le n_{n,g,t}\bar{P}^{\mathrm{sr}^+}_g, \forall g,t \tag{17}$$

$$p_{n,g,t} \le n_{n,g,t}\cdot \bar{P}_g\left(1 - \left(\mathscr{F}_g + \mathscr{P}_g(1-\upsilon_g)\right)\right), \forall g,t \tag{18}$$

$$p_{n,r,t} + p^{\mathrm{c}}_{n,r,t} = \tilde{P}^{\mathrm{R}}_{n,r,t}, \forall r,t \tag{19}$$

$$p_{n,h,t} \le \bar{P}_h \cdot n_{n,h,t}\cdot \Gamma_{n,h,w}, \forall h,t,w \tag{20}$$

$$\sum\nolimits_{t\in\mathcal{T}_\omega} p_{n,h,t} \le \mathrm{NT}\cdot \bar{P}_h\cdot n_{n,h,t}\cdot \Xi_{n,h,w}, \forall h,t,w \tag{21}$$

Storage system operation: $\forall n \in \mathcal{N}, e \in \mathcal{E}$

$$p^{\mathrm{ch}}_{n,e,t} \le \left(1-\mu_{n,e,t}\right)\cdot \bar{P}^{\mathrm{ch}}_e, \forall t \tag{22}$$

$$p^{\mathrm{dch}}_{n,e,t} \le \mu_{n,e,t}\cdot \bar{P}^{\mathrm{dch}}_e, \forall t \tag{23}$$

$$p^{\mathrm{pr}^+}_{n,e,t} + p^{\mathrm{sr}^+}_{n,e,t} \le \mu_{n,e,t}\bar{P}^{\mathrm{dch}}_e - p^{\mathrm{dch}}_{n,e,t} + p^{\mathrm{ch}}_{n,e,t}, \forall t \tag{24}$$

$$p^{\mathrm{pr}^-}_{n,e,t} + p^{\mathrm{sr}^-}_{n,e,t} \le \left(1-\mu_{n,e,t}\right)\bar{P}^{\mathrm{ch}}_e + p^{\mathrm{dch}}_{n,e,t} - p^{\mathrm{ch}}_{n,e,t}, \forall t \tag{25}$$

$$p^{\mathrm{pr}^-}_{n,e,t}, p^{\mathrm{pr}^+}_{n,e,t} \le \bar{P}^{\mathrm{pr}}_e, \forall t \tag{26}$$

$$e^{\mathrm{E}}_{n,e,t} = \eta^{\mathrm{ch}}_e p^{\mathrm{ch}}_{n,e,t} - \frac{p^{\mathrm{dch}}_{n,e,t}}{\eta^{\mathrm{dch}}_e} + e^{\mathrm{E}}_{n,e,t-1}, \forall t : t > 1 \tag{27}$$

$$\underline{E}_e \le e^{\mathrm{E}}_{n,e,t} \le \bar{E}_e, \forall t \tag{28}$$

$$p^{\mathrm{pr}^+}_{n,e,t}\mathrm{T}^{\mathrm{pr}} + p^{\mathrm{sr}^+}_{n,e,t}\mathrm{T}^{\mathrm{sr}} \le e^{\mathrm{E}}_{n,e,t} - \underline{E}_e, \forall t \tag{29}$$

$$p^{\mathrm{pr}^-}_{n,e,t}\mathrm{T}^{\mathrm{pr}} + p^{\mathrm{sr}^-}_{n,e,t}\mathrm{T}^{\mathrm{sr}} \le \bar{E}_e - e^{\mathrm{E}}_{n,e,t}, \forall t \tag{30}$$

DER operation and services: $\forall n \in \mathcal{N}, d \in \mathcal{D}$

$$\kappa_{n,d,t} = \tilde{\kappa}_{n,d,t} + \gamma^{\mathrm{shup}}_{n,d,t} - \gamma^{\mathrm{shdn}}_{n,d,t} - \gamma^{\mathrm{red}}_{n,d,t}, \forall t \tag{31}$$

$$e^{\mathrm{sh}}_{n,d,t} = \gamma^{\mathrm{shdn}}_{n,d,t}\cdot(1+\zeta_d) - \gamma^{\mathrm{shup}}_{n,d,t} + e^{\mathrm{sh}}_{n,d,t-1}, \forall t \tag{32}$$

$$e^{\mathrm{shup}}_{n,d,t} = (1+\zeta_d)\cdot e^{\mathrm{shdn}}_{n,d,t}, \forall t : t \bmod \mathrm{T}^{\mathrm{rec}}_d = 0 \tag{33}$$

$$e^{\mathrm{shup/shdn}}_{n,d,t} = e^{\mathrm{shup/shdn}}_{n,d,t-1} + \gamma^{\mathrm{shup/shdn}}_{n,d,t}, \forall t : t > 1 \tag{34}$$

$$0 \le \gamma^{\mathrm{shup/shdn/red}}_{n,d,t} \le \bar{\gamma}^{\mathrm{shup/shdn/red}}_d z^{\mathrm{D}}_{n,d}, \forall t \tag{35}$$

Transmission line limits: $\forall n \in \mathcal{N}, l \in \mathcal{L}$

$$-\underline{F}_{l,t} z^{\mathrm{L}}_{n,l} \le f_{n,l,t} \le \bar{F}_{l,t} z^{\mathrm{L}}_{n,l}, \forall t \tag{36}$$

$$f_{n,l,t} + f^{\mathrm{p}}_{n,l,t} = \bar{F}_{l,t} z^{\mathrm{L}}_{n,l}, \forall t \tag{37}$$

$$f_{n,l,t} - f^{\mathrm{n}}_{n,l,t} = -\underline{F}_{l,t} z^{\mathrm{L}}_{n,l}, \forall t \tag{38}$$

Model: Operational and investment modelling for power system planning (C)

Unit-commitment constraints: $\forall n \in \mathcal{N}, g \in \mathcal{G}$

$$n_{n,g,t} - n_{n,g,t-1} = \delta^{\mathrm{sup}}_{n,g,t} - \delta^{\mathrm{sdn}}_{n,g,t}, \forall t > 1 \tag{39}$$

$$n_{n,g,t} \ge \sum\nolimits_{\tau=t-\mathrm{T}^{\mathrm{up}}_g}^{t} \delta^{\mathrm{sup}}_{n,g,\tau}, \forall t \tag{40}$$

$$n_{n,g,t} \le \mathrm{N}_{n,g} - \sum\nolimits_{\tau=t-\mathrm{T}^{\mathrm{sdn}}_g-\mathrm{T}^{\mathrm{sup}}_g-\mathrm{T}^{\mathrm{dn}}_g}^{t} \delta^{\mathrm{sdn}}_{n,g,\tau}, \forall t \tag{41}$$

$$p_{n,g,t} - p_{n,g,t-1} \le n_{n,g,t-1}\cdot \mathrm{R}^{\mathrm{up}}_g + \delta^{\mathrm{sup}}_{g,t}\cdot \underline{P}_g, \forall t \tag{42}$$

$$p_{n,g,t-1} - p_{n,g,t} \le n_{n,g,t-1}\cdot \mathrm{R}^{\mathrm{down}}_g + \delta^{\mathrm{sdn}}_{n,g,t}\cdot \underline{P}_g, \forall t \tag{43}$$

$$\delta^{\mathrm{sup}}_{n,g,t} - \delta^{\mathrm{sdn}}_{n,g,t} \le \mathrm{N}_{n,g}\cdot v_{n,g,t}, \forall t \tag{44}$$

$$n_{n,g,t} \le \mathrm{N}_{n,g}\cdot v_{n,g,t}, \forall t \tag{45}$$

Allocation of system reserves: $\forall n \in \mathcal{N}, a \in \mathcal{A}$

$$\Omega^{\mathrm{pr}^{ty}}_{n,a,t} = \sum\nolimits_{\bar{g}\in\mathcal{G}_a} p^{\mathrm{pr}^{ty}}_{n,\bar{g},t} + \sum\nolimits_{\bar{e}\in\mathcal{E}_a} p^{\mathrm{pr}^{ty}}_{n,\bar{e},t}, \forall t, ty \tag{46}$$

$$\Omega^{\mathrm{sr}^{ty}}_{n,a,t} = \sum\nolimits_{\bar{g}\in\mathcal{G}_a} p^{\mathrm{sr}^{ty}}_{n,\bar{g},t} + \sum\nolimits_{\bar{e}\in\mathcal{E}_a} p^{\mathrm{sr}^{ty}}_{n,\bar{e},t}, \forall t, ty \tag{47}$$

$$\Delta p^{\text{g-loss}}_{n,a,t} \ge p_{n,\bar{g},t}, \forall \bar{g}, t \tag{48}$$

$$\bar{D}_{n,a,t} = D_{n,a,t} - \mathrm{LL}_{n,a}, \forall t \tag{49}$$

$$\Omega^{\mathrm{pr}^+}_{n,a,t} \ge \Delta p^{\text{g-loss}}_{n,a,t} + \sigma_a D_{n,a,t}\Delta f^{\mathrm{qssf}^-}, \forall t \tag{50}$$

$$\Omega^{\mathrm{pr}^-}_{n,a,t} \ge \mathrm{LL}_{n,a} - \sigma_a \bar{D}_{n,a,t}\Delta f^{\mathrm{qssf}^+}, \forall t \tag{51}$$

$$\Omega^{\mathrm{sr}^+}_{n,a,t} \ge \Delta p^{\text{g-loss}}_{n,a,t} - \sigma_a D_{n,a,t}\left|\Delta f^{\mathrm{db}}\right|, \forall t \tag{52}$$

$$\Omega^{\mathrm{sr}^-}_{n,a,t} \ge \mathrm{LL}_{n,a} - \sigma_a \bar{D}_{n,a,t}\left|\Delta f^{\mathrm{db}}\right|, \forall t \tag{53}$$

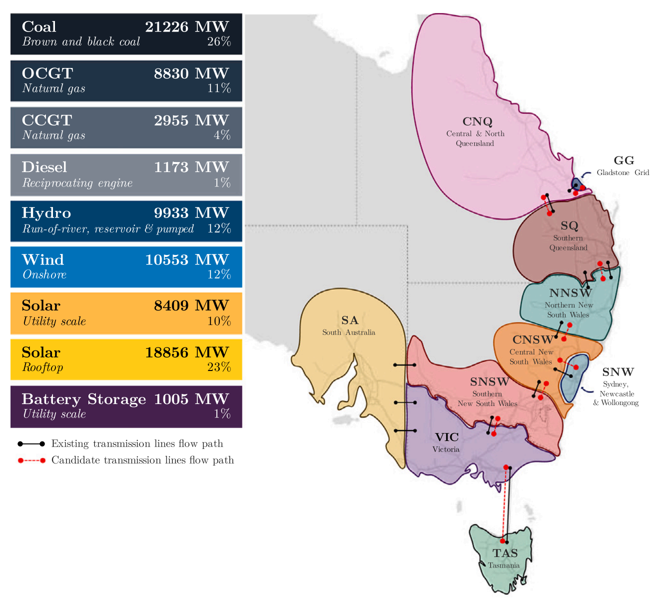

Fig. 4. Sub-regional topology of the National Electricity Market (NEM), Australia. Existing and candidate transmission line flow paths are in black and red, respectively. Boxed parameter values correspond to the system-wide installed capacity in the year 2022 for each technology. (For interpretation of the references to colour in this figure legend, the reader is referred to the web version of this article.).

3. System characterisation and input data

3.1. General overview of the system

Case study applications are undertaken in an instance of the Australian NEM, which has been divided into ten sub-regions by the system operator for planning purposes [37]. This partitioning constitutes the system model used for the studies. Fig. 4 illustrates the topology of the system, existing generation, storage and transmission corridors, as well as corridors with available expansion options.

For each scenario, existing and forecast generation and ESS capacity, expected deployment of DER, retirement of coal-fired units, and investment and fuel costs are obtained from AEMO's 2022 ISP. A clustered unit commitment approach [40] reduces the number of generators to 59, comprising 304 units across the system. Table 1 describes the techno-economic parameters of generators for the year 2022.

Table 1
Techno-economic parameters of synchronous generators [37].

Technology	Coal	Hydro	OCGT	CCGT	Diesel
Number of units	48	104	85	19	22
Variable cost ($/MWh)	13–30	7.5	117–181	64–100	127–478
Start-up costs (k$)	27–57	–	0.4–6.5	12–46	–
Rated power (MW)	280–744	15–144	33–219	48–385	31–114
Forced outage rate (pu)	0.76–0.86	0.97	0.93–0.94	0.95	0.93
Min. stable gen. (MW)	110–330	3–29	11–72	20–190	6–22
Ramp rate (MW/min)	4–8	–	3–7	2–11	–
Min up time (h)	8–16	–	–	4–6	–

The VoLL and discount rate considered for the studies are 15,000 A$/MWh,[3] and 10 % [37], respectively. The QSSF target for a generator loss is 49.5 Hz. The system's largest single generation and load losses are 744 MW and 300 MW, respectively. For existing BESS, the round-trip efficiency is 81 %, while for PHES, it is 70 %.

To study the impact and value of DER flexibility, we consider two operational modes: coordinated and non-coordinated. The coordinated DER modelling assumes active market participation (i.e., DER operational variables are part of the optimisation), while the non-coordinated approach represents a behind-the-meter setting (i.e., fixed demand-side profiles). In the coordinated approach, distributed energy storage is represented as a VPP operated by an aggregator. The demand-side participation scheme comprises four load reduction bands for limited peak shaving, with costs ranging between 300, 500, 1000 and 7500 A$/MWh. Forecast capacities of aggregated flexible DER, obtained from AEMO, are outlined in Fig. 5. Fig. 6 illustrates DER deployment trends for each scenario, highlighting the significant variability across different plausible scenarios designed by the system planner.

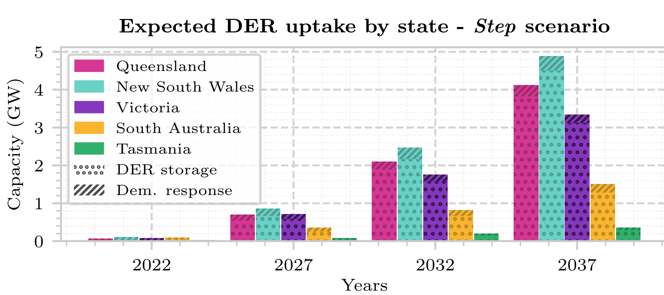

Fig. 5. State-wide disaggregation of expected DER uptake of the studied flexible DER in AEMO's *Step* scenario [37].

3.2. Investment parameters

Table 2 summarises the parameters of transmission candidate options. We consider 34 real projects from the 2022 ISP. Each investment option offers different transfer capacities between regions, with corresponding overnight capital costs detailed in the parameter ranges. We consider a 5-year lead time for deploying these lines, i.e., the period between making the investment decision and the asset becoming operational.

4. Results and discussion

In this section, we present the case study applications to illustrate the features of the proposed model and determine the value and influence

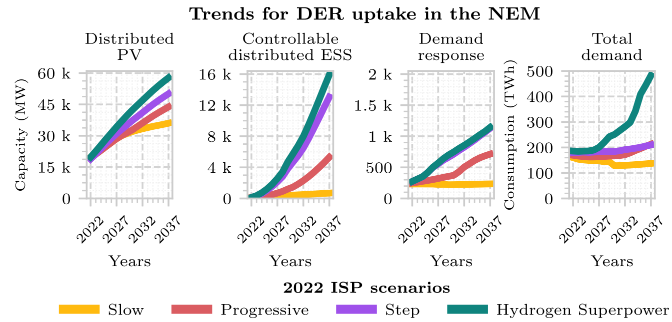

Fig. 6. 15-year forecast for DER uptake and total annual demand in AEMO's 2022 ISP scenarios. Coordinated distributed ESS corresponds to the capacity that is modelled as a VPP.

Table 2
Ranges of parameters of candidate transmission lines [37].

Reg. A	Reg. B	N° options	Transfer limits (MW)		Cap. Cost ($M/MW)
			A to B	B to A	
CNQ	GG	1	550	500	0.74
SQ	CNQ	3	0–1500	300–1500	0.18–1.08
NNSW	SQ	3	550–1800	800–2000	0.48–1.56
CNSW	NNSW	11	585–2750	470–2750	0.18–2.72
CNSW	SNW	6	600–5000	0–5000	0.18–3.76
SNSW	CNSW	3	2000–2200	2000–2200	0.48–1.51
VIC	SNSW	5	1930–2000	1500–2000	1.16–1.52
TAS	VIC	2	750	750	1.87–3.17

of DER coordination in risk-aware transmission planning under uncertainty. For each case study, we obtain investment plans, system costs, and relevant metrics such as $\text{CVaR}_{1-\alpha}$ for several levels of risk aversion β, considering a shortfall probability of $1-\alpha = 5$ %. To study the implications and benefits of DER demand-side flexibility, we obtain the aforementioned metrics for two DER operational modes previously described in Section 3.1: coordinated and non-coordinated. Risk aversion levels range from $\beta = 0$ (minimisation of total expected cost only, i.e., risk-neutral planner) to $\beta = 1$ (minimisation of CVaR only, i.e., fully risk-averse planner). The different instances of the model have been fully implemented using Julia 1.9 and JuMP. Solving has been done through Gurobi 11 via the University of Melbourne's *Spartan* High-Performance Computing services. For reference, we employ a 1 % MIPGap. The largest solved instance contains approximately 16 million constraints and 21 million variables, of which 2200 are binary and correspond to investment decisions.

4.1. Case study #1: Australia's integrated system plan

This section presents the case study applying the proposed planning framework in Australia's National Electricity Market. Fig. 7 illustrates the multi-stage scenario tree adopted for this case study. The tree spans a 20-year planning horizon, aligning with the planning horizon assessed by AEMO. We consider $|\mathcal{S}| = 4$ decision stages, justified due to the lead time associated with transmission lines. As we assume that these projects take 5 years to be deployed, four decision stages spanning across twenty years allow capturing the optionality to commit or delay investments. The tree is comprised of $|\mathcal{N}| = 32$ nodes, which is the number of nodes resulting from applying the incremental approach to create intermediate scenarios outlined in the Section 2.1.

The tree structure is based on AEMO's 2022 transmission planning scenarios: Slow, Progressive, Step, and Hydrogen Superpower,

[3] Australian dollar (A$) per MWh not served.

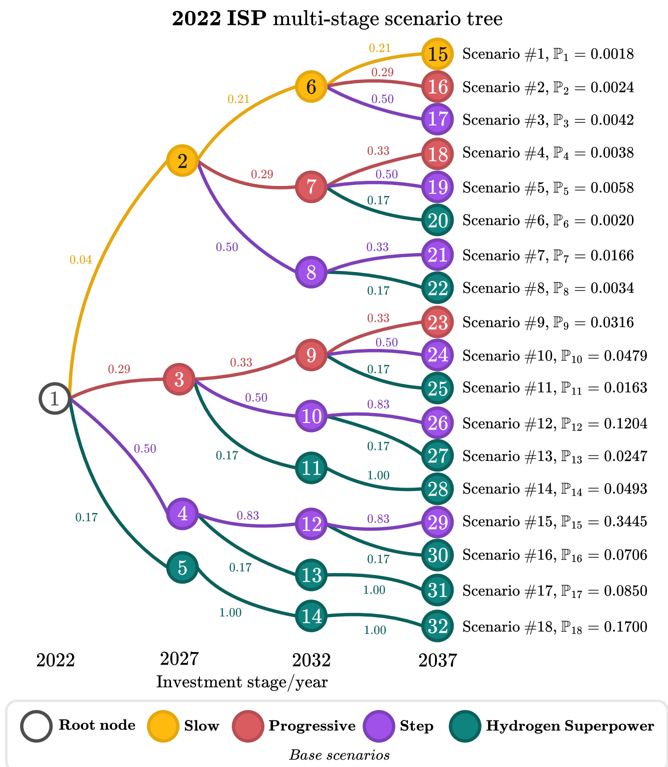

Fig. 7. Multi-stage stochastic scenario tree based on 2022 AEMO ISP. The tree can be disaggregated into 18 scenarios, each with a given probability $\mathbb{P}_s$. For example, scenario $\psi = 9$ has a probability $\mathbb{P}_9 = 0.0316$, which is obtained with the probability ρ_n of each corresponding node $\mathcal{N}_{\psi=9} = \{1, 3, 9, 23\}$, that forms the scenario within the scenario tree.

with respective probabilities[4] of 4 %, 29 %, 50 %, and 17 % [37]. These scenarios encapsulate various long-term uncertainties, including load growth, VRE and DER uptake (see Fig. 6), ESS deployment, coal-fired unit decommissioning, and fuel and investment costs. To enhance the uncertainty representation and model transitions between scenarios [27], we developed $|\Psi| = 18$ "intermediate" scenarios founded on the base scenarios. We calculated node transition probabilities ρ_n using an approach based on the base scenarios' probabilities [9]. The tree parameters and shape are illustrative and can be modified to reflect different planning perspectives.

4.1.1. Effect of DER coordination in mitigating tail risks

To illustrate the economic impact of DER coordination in risk-aware planning under uncertainty, Fig. 8 shows the distribution of total scenario costs and their cumulative probability for four levels of risk aversion β, with a shortfall probability of 5 % ($1 - \alpha = 5$ %). On the right side of each of the eight sub-figures, it is clear to distinguish the tail of each cost distribution, highlighting the behaviour of the most expensive scenarios. The figure shows the performance of costs under specific risk aversion levels (parameter β) that best demonstrate the key differences and features of the proposed planning framework in understanding the value of DER coordination.

Under a risk-neutral planning position (only expected cost minimisation, $\beta = 0$), DER coordination leads to a reduction of total expected costs of 3.4 bn, compared to the case without coordination (the reduction of expected costs comprises capital and operational costs of the system across scenarios). Remarkably, $\text{CVaR}_{5\,\%}$ is reduced by 5 bn., from 37.1 bn. to 32.1 bn when performing the same comparison. Although in this risk-neutral case, the planner is not explicitly minimising CVaR, the endogenous incorporation of long-term uncertainties in the decision-making, linked to the potential materialisation of risky scenarios, allows for exploiting DER flexibility by maximising its utilisation in worst-case scenarios. At the same time, investments in transmission are deferred, stressing the fact that sufficient DER operational flexibility could avoid lock-in to large-scale investments, potentially needed only in the materialisation of tail scenarios. Hence, through the proposed risk-aware stochastic planning framework, it is possible to develop an investment portfolio that not only minimises the expected costs but also leverages the operational flexibility available from DER coordination to hedge against the riskiest scenarios across stages.

When the planner adopts a mixed position (explicit risk and cost minimisation), as in $\beta = 0.5$, CVaR drops from 35.8 bn. to 31.4 bn. by exploiting the increased operational flexibility provided by DER coordination. Interestingly, expected total costs remain stable at 27.7 billion, consistent with the risk-neutral case. This shows that under a mixed cost-risk planning position, enabling DER coordination could help mitigate tail risks without incurring significant premiums required for additional investments. Nevertheless, it is important to note that the net CVaR reduction achieved by enabling DER coordination in the mixed cost-risk minimisation settings is lower (4.4 bn. for $\beta = 0.5$ and 4.8 bn. for $\beta = 0.99$) than in the risk-neutral setting (5 bn.). This is explained by the fact that regardless of the DER coordination mode (non-coordinated or coordinated), the planner explicitly seeks a joint cost-CVaR minimisation, forcing the portfolio of investments to reduce CVaR further and incur additional expenses. This finding suggests that a risk-neutral planner could make the most net economic benefits by leveraging DER coordination. However, a mixed cost-risk position reaches a better overall economic performance for the whole system, achieving the same expected costs but with a lower CVaR.

For a pure tail risk minimisation position ($\beta = 1$), as shown in Fig. 8, the total cost distribution is even across all scenarios for each coordination mode. This occurs because, under total risk aversion, the planner only minimises costs for the most expensive scenarios, reaching 5 % probability (scenarios 9 and 13 after the optimisation). The results suggest that DER coordination remains beneficial under this pure CVaR minimisation approach, achieving a value of 31.3 bn., the lowest across all cases. However, this comes at a premium: the system's expected cost equals the CVaR because the objective function explicitly optimises only the 5 % costlier, worst-performing scenarios.

4.1.2. Influence of DER coordination on transmission portfolios under risk aversion

Another critical aspect to investigate is the influence of flexibility from DER coordination on the decision-making regarding transmission line investments across multiple stages under different levels of risk aversion. Fig. 9 illustrates the distribution of capacity investments across scenarios for each stage, DER coordination mode, and level of risk aversion. Fig. 9a presents the risk-neutral case, while Fig. 9b–d showcase the additional capacity investments required when the planner shifts from being risk-neutral ($\beta = 0$) to different levels of risk aversion $\beta \in \{0.5, 0.99, 1\}$. For example, in a risk-neutral position ($\beta = 0$), in the year 2037, the system requires between 6 to 15 GW of additional capacity across scenarios for the non-coordinated DER mode, compared to the 5 to 11 GW required when DER are coordinated. In Fig. 9b, in year 2027, for the non-coordinated DER mode, 1 GW of additional investments would be required at a risk-aversion level of $\beta = 0.5$. This interpretation can be similarly applied to understand the results for subsequent levels of risk aversion, as shown in Fig. 9c and d.

For decision-makers, it is crucial to understand how the timing and capacity of transmission investments change under multiple uncertainties, including DER uptake, as well as the dependence of investment decisions on the level of risk aversion. As noted in Fig. 9a, in a risk-neutral context, DER coordination can significantly reduce the upper bound of the distribution of transmission investments by up to 4 GW

[4] AEMO employs these scenario probabilities to conduct an ex-post cost-benefit analysis over investment plans obtained via deterministic scenarios.

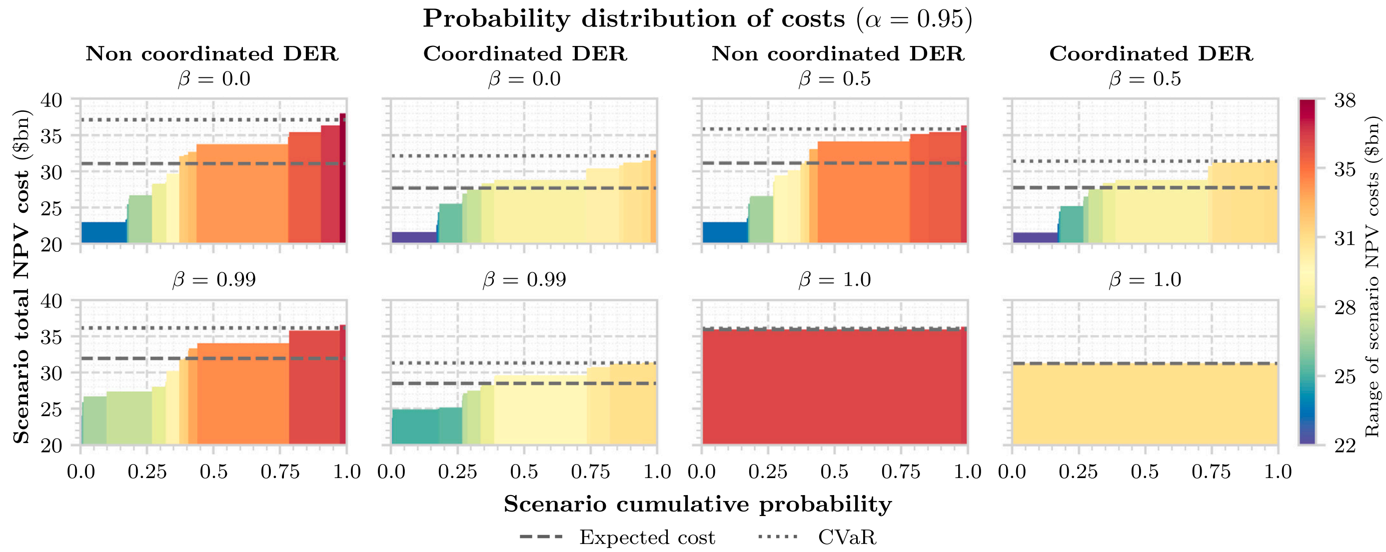

Fig. 8. Scenario-cumulative probability distribution of costs for non-coordinated and coordinated DER operational modes. Four levels of risk aversion are considered: $\beta = 0$ (risk-neutral), $\beta \in \{0.5, 0.99\}$ (mixed cost-risk position), and $\beta = 1$ (fully risk-averse), with a confidence level of $\alpha = 0.95$ (5 % shortfall probability). Expected total cost and $\text{CVaR}_{5\,\%}$ of the distribution are dashed and dotted lines, respectively. Colorbar illustrates the relative cost of each scenario compared to all scenarios in every case.

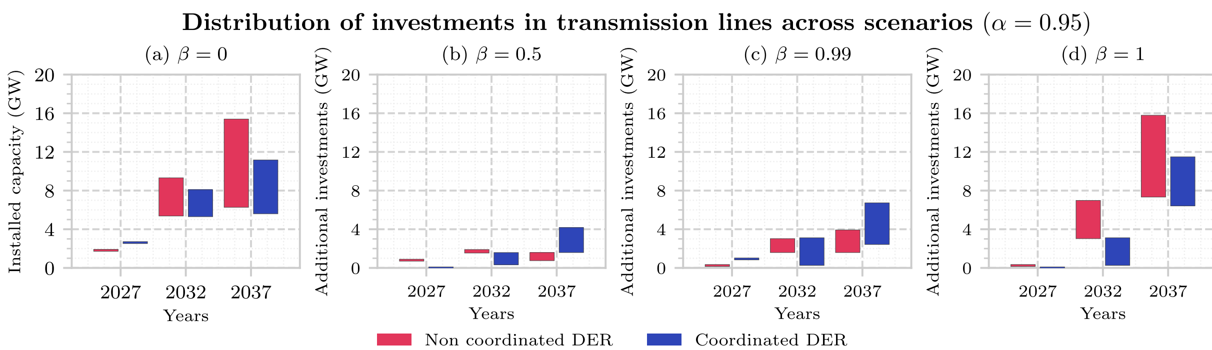

Fig. 9. Distribution of transmission line investments across scenarios for each investment stage and DER operational mode for a confidence level $\alpha = 0.95$. Subfigure (a) shows the distribution of transmission investments made in a risk-neutral setting ($\beta = 0$). Subfigures (b)–(d) illustrate the distribution of additional investments made when progressing from risk neutrality, $\beta = 0$, to different positions of risk aversion: $\beta = 0.5$, 0.99 and 1, respectively.

in stages when greater flexibility is anticipated (specifically 2032 and 2037, as indicated in Fig. 6). Consequently, DER coordination leads to a less variable portfolio across scenarios, ultimately bringing increased robustness to the decision-making tasks conducted by the planner.

Through Fig. 9b and c it is possible to analyse the behaviour of investment portfolios obtained with a shared target between minimising cost and risk. First, with the proposed risk-aware planning framework, planners are able to make reliable here-and-now decisions regarding additional investments that could be required if a risk-averse position is adopted. As shown, under different risk positions, varying values of additional installed capacity are suggested, highlighting the non-linearity of portfolios the model can capture. In later stages, as risk aversion increases, the system will require more transmission capacity for both DER coordination modes. Notably, higher transmission investments appear to be needed in the coordinated DER mode. This is explained because less capacity was installed in the risk-neutral case, given the operational flexibility provided by DER to significantly defer the building of new assets, as depicted in Fig. 9a. This suggests that with a shift to risk-averse planning, additional transmission capacity is necessary to hedge against the scenarios with lower DER uptake (like scenario 9) or higher uncertainty (such as scenario 13), those which, in fact, form the tail of the cost distribution.

In the case of a fully risk-averse planner, as illustrated in Fig. 9d, the trend observed in the previous cases changes. In this case, the model optimises a portfolio to achieve the best system performance in the worst-case scenarios with a probability of up to 5 %. Accordingly, the additional investments in 2037 for the non-coordinated case are between 7 and 16 GW; for the case with coordinated DER, this range is between 6 and 11 GW. These varying bounds emphasise the advantages of coordinated DER in allowing for a less variable and more robust investment plan in the short- and long-term in the face of potentially more conservative risk positions. Moreover, even in worst-case scenarios, coordination allows for the reduction of large-scale investments that could become inefficient.

Overall, in light of significant uncertainty and potentially lower DER uptake, additional investments in transmission could serve as a hedge for planners. This is because the expected uptake of DER in each scenario is based on forecasts from the system operator (as shown in Fig. 6), and no further investments in DER are possible. However, as illustrated in Fig. 8, DER coordination still results in simultaneously lower total costs and CVaR across all scenarios compared to a system without coordination. Ultimately, it can be emphasised that despite uncertainties concerning DER coordination and scenarios with low uptake, strong synergies and complementarity exist between transmission investments and the operational flexibility DER coordination provides at any level of risk aversion. Results highlight the ability of DER coordination to maintain the system costs significantly lower in all scenarios against a case with no coordination.

4.2. Case study #2: role of DER under a constrained supply chain and social licence issues for transmission development

The development of transmission infrastructure in power systems worldwide, and particularly in Australia, faces two significant challenges: a constrained supply chain and the need to earn social licence [37]. These factors create significant uncertainty and associated risks when planning the electricity system. Supply chain limitations and heightened social licence requirements could substantially increase capital expenditures and, consequently, overall system costs. On the other hand, construction delays caused by extended times needed to obtain social licence could also prevent the timely integration of renewable energy generation, which could be developed faster than the necessary transmission infrastructure. This situation could result in non-negligible curtailment, congestion, and a decrease in the pace of the energy transition.

In this context, DER coordination presents a viable option for enhancing the operation of the system amid uncertainties related to the decision-making and deployment of new large-scale transmission infrastructure. DER coordination could increase the system's flexibility, enabling it to locally accommodate more renewable energy while lowering peak load during critical hours, thereby reducing capital costs through the delay or deferral of capital-intensive infrastructure investments. Hence, this case study examines how DER coordination could benefit long-term system planning by potentially avoiding or hedging against economic threats from risky scenarios arising from increased capital costs and prolonged lead times in developing large-scale infrastructure.

For this analysis, we have chosen the **Step** scenario, which stakeholders identified as the most likely in AEMO's 2022 ISP. On top of it, we developed two sub-scenarios based on AEMO's assessments regarding supply chain constraints and social licence issues related to the delivery of transmission projects. We named these two sub-scenarios $\textbf{Step}^{\text{CSL}^+}$ and $\textbf{Step}^{\text{CSL}^{++}}$, representing more extreme yet plausible futures in terms of increased infrastructure costs and extended lead times. $\textbf{Step}^{\text{CSL}^+}$ assumes up to 50 % increase in capital costs for candidate transmission projects compared to the **Step** scenario. $\textbf{Step}^{\text{CSL}^{++}}$ represents a low-probability, more constrained, and pessimistic future where capital costs for candidate transmission projects increase by up to double the initial estimates. In this scenario, lead times consist of two investment stages rather than the one-stage lead time assumed in the other two scenarios. Hence, if infrastructure is decided to be built in the first investment stage, in the $\textbf{Step}^{\text{CSL}^{++}}$ scenario, it will only become operational in the third stage. To support and illustrate our assumptions regarding the feasibility of the modelled scenarios, Fig. 10 shows the distribution of capital costs per unit of additional transfer capacity (MW) across the 34 candidate transmission projects under assessment (as detailed in Table 2). The figure reveals a varied and incremental distribution of investment costs across the projects, which increase significantly in the $\textbf{Step}^{\text{CSL}^{++}}$ scenario. This highlights the considerable uncertainty regarding the final capital expenditure that planners face when determining which new transmission projects should proceed to construction.

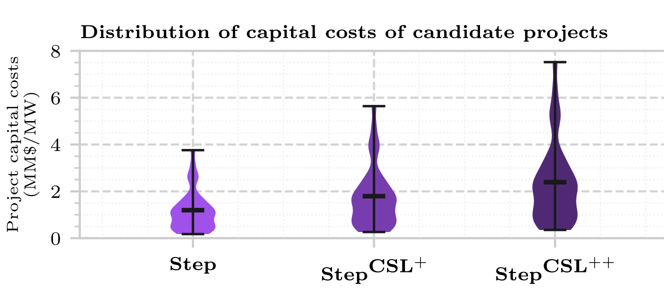

Fig. 10. Distribution of capital costs per power unit for the set of candidate projects and scenarios considered in the case study.

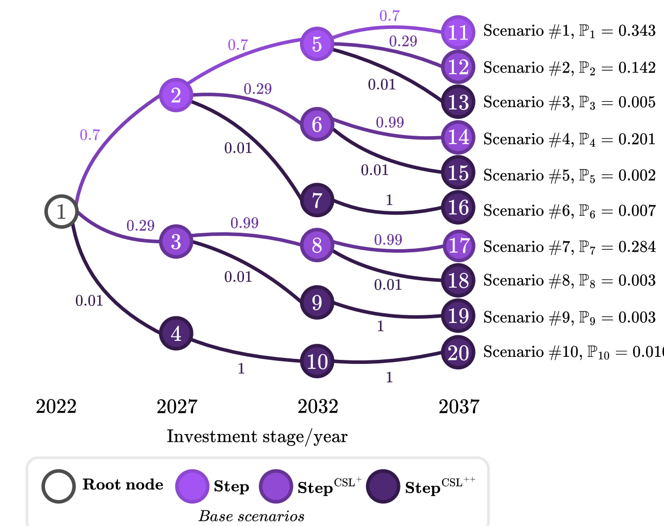

Fig. 11. Multi-stage stochastic scenario tree employed in the supply chain and social licence case study (CSL). The tree can be disaggregated into ten scenarios, each with a given probability $\mathbb{P}_s$. For example, scenario $\psi = 1$ has a probability $\mathbb{P}_1 = 0.343$, which is obtained with the probability ρ_n of each corresponding node $\mathcal{N}_{\psi=1} = \{1, 2, 5, 11\}$, that forms the scenario within the scenario tree.

Building upon cost assumptions shown in Fig. 10 and lead time considerations, Fig. 11 illustrates the scenario tree for this case study. The tree spans a 20-year planning horizon with $|\mathcal{S}| = 4$ decision stages, each representing five-year intervals corresponding to transmission infrastructure lead times. This structure allows for a systematic evaluation of investment timing, considering both immediate deployment and deferral options.

The tree is further constructed using the incremental scenario approach described in Section 2.1 and employing base scenarios **Step**, $\textbf{Step}^{\text{CSL}^+}$ and $\textbf{Step}^{\text{CSL}^{++}}$. The application of this method results in a decision tree with $|\mathcal{N}| = 20$ nodes and $|\mathcal{S}| = 10$ scenarios. Probabilities ρ_n assigned to each node have been meticulously selected to create a set that includes both plausible and low-probability scenarios. All input data related to demand, deployment of VRE, storage and DER, as well as the retirement of coal-fired generation, are consistent with the **Step** scenario across the three designed sub-scenarios. The technical parameters of the system are those outlined in Section 3.1.

To quantify the value of DER coordination flexibility under different risk aversion levels, we analyse its impacts by comparing two operational modes: coordinated and non-coordinated, subject to the uncertainties modelled in the scenario tree of Fig. 11. In applying the proposed planning framework, we set a shortfall probability $1 - \alpha = 0.05$ and considered five levels of planner risk aversion: $\beta = \{0.0, 0.5, 0.75, 0.99\}$. Table 3 summarises key numerical results, including expected total and investment costs, $\text{CVaR}_{5\,\%}$ and the capacity investments in the first stage, i.e., the amount of transmission that should start to be developed *here-and-now*. Fig. 12 illustrates the cost probability distribution obtained for each case and coordination mode. In each sub-figure, we compare performance based on expected costs, $\text{CVaR}_{5\,\%}$, and costs per scenario. Each circle in the probability distribution represents the total costs for each scenario.

From Table 3, it is important to highlight that the savings in expected costs achievable through DER coordination are 3.8 bn., regardless of the level of risk aversion. In terms of $\text{CVaR}_{5\,\%}$, these increase to a range between 3.9 and 4.2 bn. across cases. This trend is further illustrated in Fig. 12, where the flexibility offered by DER coordination leads to improved performance in both metrics, emphasising the role of coordination as a buffer against scenarios characterised by significant infrastructure planning uncertainty. Remarkably, the consistent

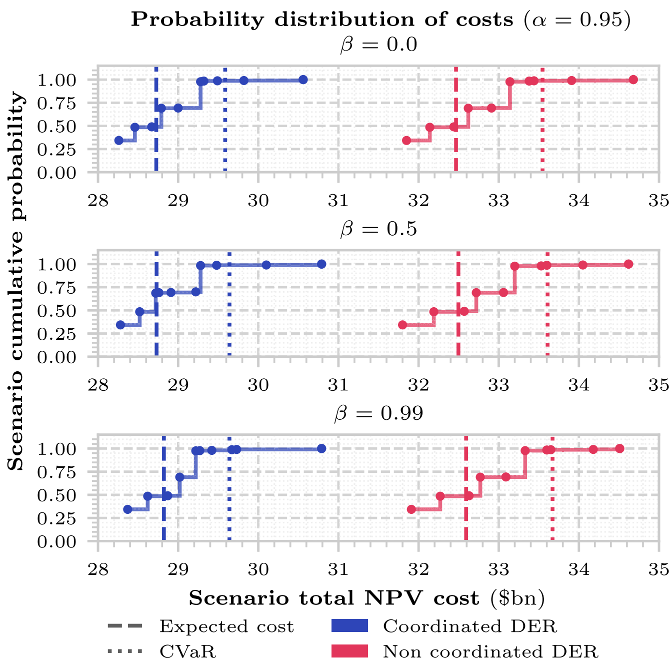

Fig. 12. Scenario-cumulative probability distribution of costs for non-coordinated and coordinated DER operational modes. We consider three levels of risk aversion: $\beta = 0$ (risk-neutral), $\beta \in \{0.5, 0.99\}$ (mixed cost-risk position), with a confidence level of $\alpha = 0.95$ (5 % shortfall probability). The expected total cost and $\text{CVaR}_{5\,\%}$ of the distribution are the dashed and dotted lines, respectively. Dots mark the exact cost of each scenario.

behaviour of these two metrics across cases highlights that the proposed methodology is able to leverage the flexibility from coordination to maximise benefits, independent of the risk position of the planner. Moreover, it is possible to identify transmission investment portfolios that synergise with such DER flexibility to maintain the techno-economic performance of the system in the face of uncertainties in capital costs and infrastructure lead times.

In terms of investment decision-making, it becomes crucial to analyse, with a real-world perspective, the impact of uncertainties considered for infrastructure development and the potential role of DER coordination. In this vein, Table 3 describes the first-stage decisions suggested by the stochastic model for different levels of risk aversion and coordination modes. First-stage, *here-and-now*, decisions indicate the infrastructure that must begin to be built today to be available in the subsequent stage, according to the lead time considered in each scenario. In a risk-neutral position ($\beta = 0$), DER coordination provides clear benefits for both expected and investment costs, although the overall decision to build new infrastructure with 1570 MW capacity remains unchanged compared to the non-coordinated mode. When examining higher degrees of risk aversion, a typical position for system planners, the portfolio of investments varies significantly. For example, at $\beta = 0.99$, without DER coordination, it is suggested to avoid any early transmission investment. This happens because the planner primarily focuses on hedging against worst-case scenarios, i.e., those with higher capital costs and longer lead times. This poses the risk of making an inefficient decision compared to the risk-neutral case (where investments are made) due to the increased concern only in low-probability scenarios.

On the other hand, when DER are coordinated, the model suggests proceeding with a 1270 MW investment, highlighting the crucial role of coordination flexibility in decision-making under uncertainty. Notably, the increased operational flexibility provided by DER coordination enables early *here-and-now* investments despite uncertainties from low-probability scenarios. This is explained by the fact that a more economical system operation can be achieved via DER coordination, leaving room to proceed with investments required early in scenarios that accumulate a higher probability. This underscores the importance of developing mechanisms to enable demand-side flexibility via DER coordination. As shown, significant benefits could be provided in order to mitigate economic shocks associated with large-scale infrastructure planning. Additionally, as shown in Table 3, the expected investment costs are still lower in each case with coordination. This indicates that coordinated DER can effectively adjust the need for early investments amid deployment and capital cost uncertainties, which may stem from a constrained supply chain or increased requirements for obtaining social licence. Overall, the findings suggest that an optimised investment portfolio can be achieved by coordinating DER and accounting for a non-zero degree of risk aversion in the face of significant investment uncertainty. Such a portfolio would not only substantially lower the risk of costlier scenarios but also maintain total expected costs at similar levels despite varying degrees of risk aversion.

5. Conclusions

In this paper, we investigated the role and techno-economic value of the coordination of distributed energy resources (DER) in the context of risk-aware power system planning under uncertainty. We introduced a multi-stage framework that employs a Conditional Value-at-Risk (CVaR)-based reformulation for risk-aware expansion planning. We applied this framework to study, for the first time, the interaction between transmission investments and DER coordination under various scenarios incorporating several long-run uncertainties and in light of varying planners' risk positions. We demonstrated the real-world applicability of the approach through various case studies in the National Electricity Market (NEM), Australia, offering planners with a comprehensive method to optimise investment portfolios under several uncertainties while controlling their risk position.

The results and analysis demonstrated that endogenously incorporating uncertainties while controlling for risk aversion in transmission planning could unlock significant economic savings through DER coordination. Notably, coordination enables simultaneous reductions in expected and tail costs under specific levels of planner risk aversion. Importantly, this key feature for system planning is only achievable through an uncertainty-aware stochastic planning framework, such as the one proposed, due to the possibility of blending many long-term uncertainties into a thoughtfully formulated incremental scenario tree.

Table 3
Summary of results for case study #2.

β	Coordination mode	Exp. Tot. Cost ($bn.)	$\text{CVaR}_{5\,\%}$ ($bn.)	Exp. Inv. Cost ($bn.)	1st stage inv. (MW)
0.0	Coordinated DER	28.7	29.6	2.6	1570
	Non coordinated DER	32.5	33.5	3.3	1570
0.5	Coordinated DER	28.7	29.6	2.7	1270
	Non coordinated DER	32.5	33.6	3.9	1270
0.75	Coordinated DER	28.7	29.6	2.8	1270
	Non coordinated DER	32.4	33.7	3.7	1270
0.99	Coordinated DER	28.8	29.6	3.0	1270
	Non coordinated DER	32.6	33.7	3.7	0

Moreover, a result of this nature would not be achievable through a deterministic (single-scenario) planning approach due to the impossibility of generating a probabilistic distribution of scenarios.

The findings of this paper could also lead to relevant and practical real-world recommendations. As shown, DER coordination proves to be a promising techno-economic option for increasing system flexibility, relieving the grid in adverse scenarios, and thus reducing overall costs while enabling a more robust, adaptive infrastructure planning and decision-making. However, to fully harness these benefits, adequate regulatory frameworks and policies are key to supporting the implementation of appropriate coordination mechanisms. Additionally, technologies capable of enabling seamless integration and visibility between DER and operators must be in place to ensure secure and reliable integrated whole-system operation.

From a decision-making perspective, in order to fully leverage the benefits of flexibility from DER coordination in managing the impact of planning-related uncertainties, proactive and adaptive infrastructure planning methods are key to adequately informing investment plans. It is highlighted that to complement any further DER development in any scenario and risk position, transmission investments remain crucial. Questions such as their timing, capacity, and location must be adequately answered in the face of long-term uncertainties. Hence, to make the right decisions, relevant stakeholders ought to adopt advanced multi-stage risk- and uncertainty-aware planning methods to represent uncertainties and hedge against the risks that arise from them. Such an approach would aid in preventing inefficient investment decisions that could lead to suboptimal infrastructure development, particularly for capital-intensive projects.

CRediT authorship contribution statement

Pablo Apablaza: Writing – review & editing, Writing – original draft, Visualization, Validation, Software, Methodology, Formal analysis, Data curation, Conceptualization. **Sebastián Püschel-Løvengreen:** Writing – review & editing, Writing – original draft, Supervision, Software, Methodology, Data curation, Conceptualization. **Rodrigo Moreno:** Writing – review & editing, Supervision, Methodology, Conceptualization. **Pierluigi Mancarella:** Writing – review & editing, Writing – original draft, Supervision, Methodology, Funding acquisition, Conceptualization.

Declaration of competing interest

The authors declare that they have no known competing financial interests or personal relationships that could have appeared to influence the work reported in this paper.

Data availability

Data used for studies is publicly available.

References

[1] G. Elizondo, R. Poudineh, Harnessing the power of distributed energy resources in developing countries: what can be learned from the experiences of global leaders? Oxford Institute for Energy Studies, Tech. Rep. 10, 2023.

[2] S. Riaz, P. Mancarella, Modelling and characterisation of flexibility from distributed energy resources, IEEE Trans. Power Syst. 37 (1) (Jan. 2022) 38–50.

[3] A. Churkin, W. Kong, J.N.M. Gutierrez, E.A.M. Ceseña, P. Mancarella, Tracing, ranking and valuation of aggregated DER flexibility in active distribution networks, IEEE Trans. Smart Grid (2023) 1.

[4] M.Z. Liu, L.N. Ochoa, S. Riaz, P. Mancarella, T. Ting, J. San, J. Theunissen, Grid and market services from the edge: using operating envelopes to unlock network-aware bottom-up flexibility, IEEE Power Energy Mag. 19 (4) (Jul. 2021) 52–62.

[5] D. Pudjianto, C. Ramsay, G. Strbac, Virtual power plant and system integration of distributed energy resources, IET Renew. Power Gener. 1 (1) (2007) 10–16.

[6] B. Mohandes, M.S.E. Moursi, N. Hatziargyriou, S.E. Khatib, A review of power system flexibility with high penetration of renewables, IEEE Trans. Power Syst. 34 (4) (Jul. 2019) 3140–3155.

[7] P. Apablaza, S. Püschel-Løvengreen, R. Moreno, S. Mhanna, P. Mancarella, Assessing the impact of DER on the expansion of low-carbon power systems under deep uncertainty, Electr. Power Syst. Res. 235 (Oct. 2024) 110824.

[8] Australian Energy Market Operator, 2024 Integrated System Plan, Tech. Rep., 2024.

[9] S. Püschel-Løvengreen, S. Mhanna, P. Mancarella, Flexible planning of low-carbon power systems under deep uncertainty, CIGRE Sci. Eng. 31 (2023).

[10] B.F. Hobbs, Q. Xu, J. Ho, P. Donohoo, S. Kasina, J. Ouyang, S.W. Park, J. Eto, V. Satyal, Adaptive transmission planning: implementing a new paradigm for managing economic risks in grid expansion, IEEE Power Energy Mag. 14 (4) (Jul. 2016) 30–40.

[11] I. Konstantelos, G. Strbac, Valuation of flexible transmission investment options under uncertainty, IEEE Trans. Power Syst. 30 (2) (Mar. 2015) 1047–1055.

[12] R. Moreno, A. Street, J.M. Arroyo, P. Mancarella, Planning low-carbon electricity systems under uncertainty considering operational flexibility and smart grid technologies, Phil. Trans. R. Soc. A: Math. Phys. Eng. Sci. 375 (2100) (Aug. 2017).

[13] C. Vartanian, R. Bauer, L. Casey, C. Loutan, D. Narang, V. Patel, Ensuring system reliability: distributed energy resources and bulk power system considerations, IEEE Power Energy Mag. 16 (6) (Nov. 2018) 52–63.

[14] I.J. Perez-Arriaga, The transmission of the future: the impact of distributed energy resources on the network, IEEE Power Energy Mag. 14 (4) (Jul. 2016) 41–53.

[15] National Grid ESO, Future Energy Scenarios: ESO Pathways to Net Zero, Tech. Rep., 2024.

[16] Réseau de Transport d'Électricité, Futurs ÉnergÉtiques 2050, Tech. Rep., 2022.

[17] International Energy Agency, Unlocking the Potential of Distributed Energy Resources, Tech. Rep., 2022.

[18] H. Wang, S. Riaz, P. Mancarella, Integrated techno-economic modeling, flexibility analysis, and business case assessment of an urban virtual power plant with multi-market co-optimization, Appl. Energy 259 (2) (2020).

[19] D. Alvarado, A. Moreira, R. Moreno, G. Strbac, Transmission network investment with distributed energy resources and distributionally robust security, IEEE Trans. Power Syst. 34 (6) (Nov. 2019) 5157–5168.

[20] D. Alvarado, R. Moreno, A. Street, M. Panteli, P. Mancarella, G. Strbac, Co-optimizing substation hardening and transmission expansion against earthquakes: a decision-dependent probability approach, IEEE Trans. Power Syst. (May 2023).

[21] J. Contreras-Ocaña, U. Siddiqi, B. Zhang, Non-wire alternatives to capacity expansion, in: IEEE General Meeting Power & Energy Society, IEEE, Portland, 2018.

[22] E.F. Alvarez, L. Olmos, A. Ramos, K. Antoniadou-Plytaria, D. Steen, L.A. Tuan, Values and impacts of incorporating local flexibility services in transmission expansion planning, Electr. Power Syst. Res. 212 (2022) 11.

[23] R. Quint, L. Dangelmaier, I. Green, D. Edelson, V. Ganugula, R. Kaneshiro, J. Pigeon, B. Quaintance, J. Riesz, N. Stringer, Transformation of the grid: the impact of distributed energy resources on bulk power systems, IEEE Power Energy Mag. 17 (6) (Nov. 2019) 35–45.

[24] A.H. van der Weijde, B.F. Hobbs, The economics of planning electricity transmission to accommodate renewables: using two-stage optimisation to evaluate flexibility and the cost of disregarding uncertainty, Energy Econ. 34 (6) (Nov. 2012) 2089–2101.

[25] L.A. Roald, D. Pozo, A. Papavasiliou, D.K. Molzahn, J. Kazempour, A. Conejo, Power systems optimization under uncertainty: a review of methods and applications, Electr. Power Syst. Res. 214 (Jan. 2023).

[26] E. Spyrou, B. Hobbs, D. Chattopadhyay, N. Mukhi, How to assess uncertainty-aware frameworks for power system planning? IEEE Trans. Energy Mark. Policy Regul. (Feb. 2024) 1–13.

[27] B. Moya, R. Moreno, S. Püschel-Løvengreen, A.M. Costa, P. Mancarella, Uncertainty representation in investment planning of low-carbon power systems, Electr. Power Syst. Res. 212 (2022) 11.

[28] J. Álvarez López, K. Ponnambalam, V.H. Quintana, Generation and transmission expansion under risk using stochastic programming, IEEE Trans. Power Syst. 22 (3) (Aug. 2007) 1369–1378.

[29] A.J. Conejo, L. Baringo, J. Kazempour, A. Siddiqui, Investment in Electricity Generation and Transmission Decision Making Under Uncertainty, 2016.

[30] R. Rockafellar, S. Uryasev, Conditional value-at-risk: optimization approach, Applied Optimization - Stochastic Optimization: Algorithms and Applications, vol. 54, 2001, pp. 411–435.

[31] F.D. Munoz, A.H. van der Weijde, B.F. Hobbs, J.P. Watson, Does risk aversion affect transmission and generation planning? A Western North America case study, Energy Econ. 64 (May 2017) 213–225.

[32] A. Inzunza, R. Moreno, A. Bernales, H. Rudnick, CVaR constrained planning of renewable generation with consideration of system inertial response, reserve services and demand participation, Energy Econ. 59 (Sep. 2016) 104–117.

[33] T. Möbius, I. Riepin, F. Müsgens, A.H. van der Weijde, Risk aversion and flexibility options in electricity markets, Energy Econ. 126 (Oct. 2023) 106767.

[34] D. Kitamura, L. Willer, B. Dias, T. Soares, Risk-averse stochastic programming for planning hybrid electrical energy systems: a Brazilian case, Energies 16 (3) (Feb. 2023).

[35] A. Xuan, X. Shen, Q. Guo, H. Sun, A conditional value-at-risk based planning model for integrated energy system with energy storage and renewables, Appl. Energy 294 (Jul. 2021).

[36] R. Moreno, M. Panteli, P. Mancarella, H. Rudnick, T. Lagos, A. Navarro, F. Ordonez, J.C. Araneda, From reliability to resilience: planning the grid against the extremes, IEEE Power Energy Mag. 18 (4) (Jul. 2020) 41–53.

[37] Australian Energy Market Operator (AEMO), Integrated system plan for the National Electricity Market, 2022.

[38] C. Truong, S. Trück, It's not now or never: implications of investment timing and risk aversion on climate adaptation to extreme events, Eur. J. Oper. Res. 253 (3) (Sept. 2016) 856–868.

[39] J.A. Schachter, P. Mancarella, Demand response contracts as real options: a probabilistic evaluation framework under short-term and long-term uncertainties, IEEE Trans. Smart Grid 7 (2) (Mar. 2016) 868–878.

[40] L. Zhang, T. Capuder, P. Mancarella, Unified unit commitment formulation and fast multi-service LP model for flexibility evaluation in sustainable power systems, IEEE Trans. Sustain. Energy 7 (2) (Apr. 2016) 658–671.